9

Flammability and fire resistance of composites

A R HORROCKS and B K KANDOLA,
University of Bolton, UK

9.1 Introduction

All fibre-reinforced composites comprise matrix materials that are flammable to varying degrees and, compared with metals such as aluminium or steel, can burn vigorously, often with evolution of smoke. While organic fibre reinforcement such as polyester, aramid and even carbon may add fuel to the burning composite, even if inorganic fibres such as E-glass are the reinforcing structures, the general composite fire resistance and performance (including smoke generation) will be determined by that of the organic matrix. The overall physical behaviour under heat and flame conditions will be influenced by the thermal properties of the fibres present since resins are often thermoplastic or deformable except in the highest performance examples such as phenolics and polyimides. Table 9.1 illustrates the thermal properties of typical fibre reinforcement for composites. It is seen that while glass fibres are probably the most commonly used fibres, while they are non-flammable, their relatively low melting point compared with typical flame temperatures of 1000 °C or so will ensure that under fire exposure conditions, glass fibre reinforced composites will start to deform when temperatures reach 500 °C and above. Thus whether or not a composite maintains both a heat and flame barrier to an advancing fire depends on the combined flammable behaviour of the fibres and resins present, coupled with their abilities to withstand the physical aspects of applied heat.

Fire resistance and smoke generation properties of composite materials are major issues these days because, depending on applications, they must pass some type of regulatory fire test in order to ensure public safety. Thus, it is important to understand how individual components of the end-products burn and how best to modify materials to make them flame-resistant without compromising their uniquely valuable low weight to high mechanical property ratios.

This chapter complements our earlier reviews [1, 3], to which the reader is directed for a greater background understanding and which have provided

Table 9.1 Physical and mechanical properties of fibres [1, 2]

Fibre	Diameter (μm)	Tensile strength (GPa)	Initial modulus (GPa)	Density (kg m^{-3})	Second order, T_g or softening temp. (°C)	Max. service temp. (°C)	Limiting oxygen index, LOI (%)
E-Glass	3–20	2–6	50–100	2400–2600	>700	250	–
S-Glass	3–20	3.5	87	2500	>700	250	–
Carbon*	4–10	1.5–7.0	150–800	1500–2000	–	400–450	55–60
Para-aramid	10	2–4	70–150	1410–1450	340	200	30
Boron	100–200	2–4	370–430	2500–2700	–	350	–
UHMWPE	10–30	1.5	70	990–1020	–50	100	18–19
Alumina	10–20	0.5	310	3800–4000	–	1000	–

*Carbon and graphite fibres.

general overviews of composite fire resistance. This chapter, while presenting a brief overview of composite fire behaviour, will focus on recent research that has concentrated on understanding resin thermal behaviour and the resins used and means of enhancing fire and smoke performance using flame retardants that do not use the environmentally and toxicologically questioned antimony–bromine-based flame retardants [4, 5].

9.2 Constituents – their physical, chemical, mechanical and flammability properties

The structures and physical and mechanical characteristics of textile reinforced composites are described elsewhere in this text, but adhesion between two dissimilar phases is necessary to allow uniform load distribution between them and the nature of the sustenance of this bond under thermal conditions is an essential determinant of the physical stability of a composite in a fire. The thermochemical and thermophysical properties of the fibres and matrix will also be significant fire performance-determining issues. Fire properties also depend upon the methods used to combine these components into one material and whether flame-retardant additives or other systems are included. Generally, there are three methods of conferring fire resistance on composites:

1. Use of inherently flame-resistant resins and/or fibres: the use of different generic resins will be discussed below, as will the thermal properties of available fibres. Modifications of the various resin types by inclusion of flame-retardant comonomers (e.g. brominated variants, particularly polyesters) is beyond the scope of this chapter and the reader is referred elsewhere [6].
2. Incorporation of flame retardant additives. These are included along with some our own recent research using intumescent materials.
3. Use of external coatings and outer protective surfaces. These are usually additional to the fundamental composite and may include paints, coatings and ceramic fibrous structures, often as wet-laid nonwoven structures which are incorporated in the surface(s) that will be fire exposed. These will also be briefly reviewed below with a focus on recent research.

9.2.1 Fibres

The main fibres are chosen from the armoury of conventional and high-performance fibres available to the textile and fibre industries in general and Table 9.1 lists the properties of those most commonly used for composites. In this table, resistance to heat and flame is given in terms of the second order, glass transition temperature (T_g), or softening temperature, the maximum

service life temperature and the burning propensity defined in terms of limiting oxygen index, LOI – the percentage of oxygen required to sustain burning of a vertical sample in a downward direction [5]. Thus the fire-resistant fibres have the highest values possible for each of these parameters. For burning, it is generally accepted that if a material has LOI > 30, then in an air atmosphere, it will be deemed to be flame retardant. Such a fibre, e.g. para-aramid, will still burn in a well-ventilated fire.

Fibrous arrays can be in the form of woven or nonwoven cloths or layers. Generally, composites will contain at best a single fibre type and occasionally two, e.g. carbon warp and aramid weft. Discontinuous fibres can also be used, e.g. chopped fibres about 30–50 mm long, distributed in a random manner in a plane and held together with a resin binder. Both tows and cloths can be pre-impregnated with resin, processed and then used as 'prepregs' during composite manufacture. Some of the most used fibres are reviewed briefly below.

Glass fibres

Based on different chemical compositions, various grades of glass are available commercially, e.g. E-, S- R- and C-glass [2]. By pulling swiftly and continuously from the melt, glass can be drawn into very fine filaments. Continuous glass fibres are $3–20 \times 10^{-6}$ m in diameter. The physical properties are given in Table 9.1 [2] and for most textile-reinforced composites E- (electrical resistance) and S- (high strength) glass fibres are preferred because of their combined properties of high strength and modulus. The advantages of glass fibres are their combination of chemical inertness and their high tensile and compressive strengths, low cost, good compatibility and good processibility. The disadvantages are associated with their low modulus and physical thermal stability. When heated, while they are flame resistant in respect of their not supporting combustion, they soften at relatively low temperatures and by 500 °C have lost most of their physical strength and so have limited temperature performance ranges.

Carbon fibres

Carbon fibres are manufactured by controlled pyrolysis and cyclisation of certain organic precursors, e.g. polyacrylonitrile (PAN). Carbon fibres have characteristics of low density, high strength and stiffness. As shown in Table 9.1, their stiffness is high compared with glass fibres. Mechanical characteristics of carbon fibres do not deteriorate with temperature increases up to 450 °C, so they can be used for both polymeric and metal matrices. They are used for manufacturing load-carrying panels of aircraft wings and fuselages, drive shafts of cars and parts operating under intense heating. At temperatures

above 450 °C, they will chemically start to oxidise and only become really combustible once temperatures approach 1000 °C.

Aramid fibres

Aramid fibres are based on aromatic polyamides, and where at least 85% of the amide groups are connected directly to an aromatic group, they are generically called aramid fibres. For composites, the para-aramids with their superior tensile properties are preferred and these are typified by the various commercial grades of Kevlar® (Du Pont), and Twaron® (AKZO) and similar fibres available. The general chemical formula for these para-aramids is typified by that for poly(*p*-phenylene terephthalamide) (PPT)

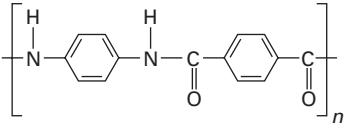

9.1

While they have excellent tensile properties, their second order transition temperatures are much higher than the majority of organic high-performance fibres (see Table 9.1) although their flammability as measured by limiting oxygen index, for example, is moderate (LOI = 30–31) and comparable with that of the meta-aramids (eg Nomex®, Du Pont) and flame-retardant cotton and wool [5].

Boron fibres

Boron fibres are obtained by high-temperature reduction of boron trichloride vapour on a tungsten or carbon substrate. With rise in temperature, fibres start to degrade in air at 400 °C. In order to prevent their oxidative degradation, they are covered with a refractory silicon or boron carbide coating. They are typically 100–200 $\times 10^{-6}$ m in diameter. Because of their large diameter and high stiffness, it is not possible to carry out normal textile processes such as weaving. Hence, these are used in the form of single-thickness, parallel-laid, pre-impregnated sheets or narrow continuous tapes [1]. Their main advantages are high stiffness and compression strength, but they are rather expensive. Table 9.1 shows that their ability to withstand working temperatures as high as 350 °C for their whole expected service lives is a significant factor in their selection for high-temperature applications.

Polyethylene fibres

Fibres from ultra-high molecular weight polyethylene (UHMWPE) may be produced to have similar tensile properties as aramids. While their hydrocarbon chains have chemical inertness, not only do they burn typically like any hydrocarbon material (LOI = 18–19) but also a second major disadvantage is their low melting point, 130–150 °C and hence low maximum service temperatures of only 100 °C or so. Examples of UHMWPE are Spectra (Allied fibres) and Dyneema (DSM).

Alumina fibres

Fibres of polycrystalline alumina can be made by extruding a thickened mixture of fine alumina powder suspended in an alginate binder and then sintering the fibrous mass at high temperature. Alumina fibres are very strong and are resistant to temperatures as high as 900–1000 °C. It may thus be deduced that as fibres, they can offer the greatest fire resistance of all used in composite markets. Examples are Nextel® (3M Corp.) and Saffil® (Saffil Ltd., UK) and they may be used with epoxy, polyimide and maleimide resins.

9.2.2 Matrix polymers

The most common matrix materials for composites (and the only ones discussed here) are polymeric, which can be thermoset or thermoplastic; examples are presented in Table 9.2. Thermoset matrices are fabricated from the respective resin, a curing agent, a catalyst or curing initiator and a solvent sometimes introduced for lowering the viscosity and improving impregnation of reinforcements. In thermosets, solidification from the liquid phase takes place by the action of an irreversible chemical crosslinking reaction which produces a tightly bound three-dimensional 3D network of polymer chains. The molecular units forming the network and the length and density of the crosslinks of the structure will influence the mechanical and any residual thermoplastic properties of the material. The level of crosslinking between resin functional groups and often the degree of non-thermoplasticity is a function of the degree of cure, which usually involves application of heat and pressure. However, some resins cure at room temperature.

The second type of polymers are thermoplastic in nature and have the advantage that they can be formed by physical processes of heating and cooling. Thermoplastics readily flow under stress at elevated temperatures, can be fabricated into required components and become solid and retain their shape when cooled to room temperature. However, the reversibility of this process generates composites having a thermoplastic property and, hence,

Table 9.2 Limiting oxygen index values for polymers and composites at 23 °C [7–9]

Resin	LOI (%)	
	Resin	40% (w/w) resin/ 181 glass cloth
Thermoplastic resins		
Acrylonitrile–butadiene–styrene	34	
Polyaryl sulphone (PAS)	36	
Polyether sulphone (PES)	40	
9,9Bis-(4-hydroxyphenyl) fluorene/ polycarbonate-poly(dimethyl siloxane) (BPFC-DMS)	47	
Polyphenylene sulphide (PFS)	50	
Thermoset resins		
Polyester	20–22	
Vinyl ester	20–23	
Epoxy	23	27
Phenolic	25	57
Polyaromatic melamine	30	42
Bismaleimide	35	60

poor physical resistance to heat. The most widely used matrix materials are discussed below along with their thermal degradative characteristics.

Polyester resins

Polyesters are probably the most commonly used of polymeric resin materials. The advantages of polyester matrices are their ability to cure over a wide range of temperatures under moderate pressures and their low viscosities providing good compatibility with fibres. In addition is their ability to be readily modified by other resins. Essentially they consist of a relatively low molecular weight unsaturated polyester chain dissolved in styrene. Curing occurs by the polymerisation of the styrene, which forms crosslinks across unsaturated sites in the polyester. Curing reactions are highly exothermic, and this can affect processing rates as excessive heat can be generated which can damage the final laminate. The general formula for a typical resin [10] is shown in Fig. 9.2. Among the drawbacks of polyester resins are poor mechanical characteristics, low adhesion, relatively large shrinkage and the presence of toxic components of the styrene type.

Most polyesters start to decompose above 250 °C, whereas the main step of weight loss occurs between 300 and 400 °C [6]. During thermal decomposition, polystyrene crosslinks start to decompose first and styrene is volatilised (Fig. 9.3). The linear polyester portion undergoes scission similar to thermoplastic polyesters (Fig. 9.4), undergoing decarbonylation,

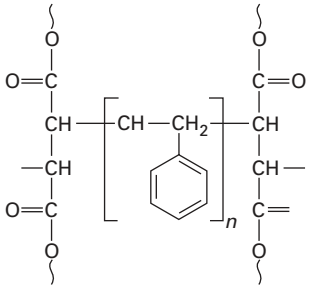

9.2

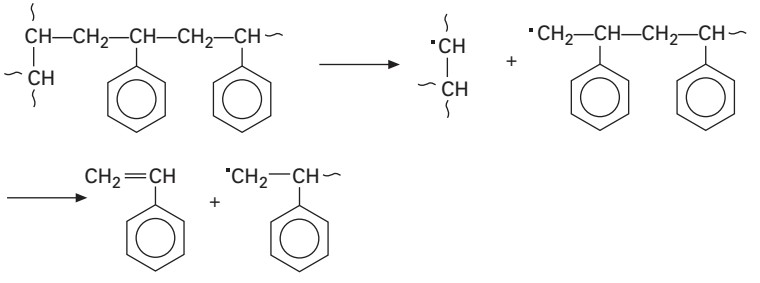

9.3

decarboxylation or splitting off of methylacetylene. Learmonth and Nesbit [11] have shown that during thermal decomposition volatiles are lost up to 400 °C and, above 400 °C, it is solid phase oxidation reactions that predominate with initial attack occurring at crosslinks [12].

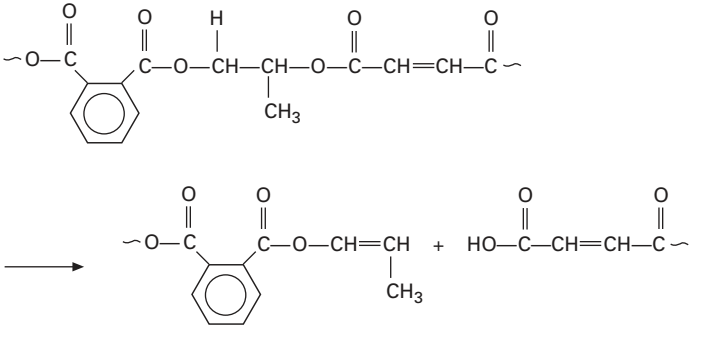

9.4

Because of the ease of formation of these flammable pyrolysis products, polyesters have LOI values of 20–22 and hence, flame readily, and sometimes vigorously, after ignition. Unsaturated polyesters, crosslinked with styrene,

burn with heavy sooting. These can be flame retarded by addition of inorganic fillers, addition of organic flame retardants, chemical modification of the acid, alcohol or unsaturated monomer component and the chemical combination of organo-metallic compounds with resins [10].

It is common practice to add inert fillers to polyester resins to reinforce the cured composite, to lower cost and to improve flame retardance. Glass fibre and calcium carbonate often increase the burning rate of the composition [10], but other fillers such as antimony trioxide for halogenated compositions and hydrated alumina are quite effective flame retardants. Modification of the saturated acid component has been by far the most successful commercial method of preparing flame-retardant unsaturated polyesters. Examples are halogenated carboxylic acids, such as chlorendic acid or their anhydrides, tetrachloro- or tetrabromophthalic anhydride [13].

Halogenated alcohols or phenol can also be incorporated into the polymeric chain. Examples are tribromo-neopentyl glycol, tetrabromobisphenol-A and dibromophenol. The crosslinking partner may also be flame-retardant, as in the case of monochloro- or dichlorostyrene and hexachloropentadiene. Examples of halogenated additive compounds are tetrabromo-*p*-xylene, pentabromobenzyl bromide, pentabromoethyl benzene, pentabromotoluene, tribromocumene, decabromodiphenyl oxide and brominated epoxy resins [13]. The effectiveness of halogenated components is enhanced by simultaneous addition of antimony trioxide.

Phosphorus-containing flame retardants such as phosphonates and dialkyl phosphites can be incorporated into the polyester chain. In addition, allyl or diallyl phosphites may act as crosslinking agents [13].

Vinyl ester resins

Vinyl ester resins like unsaturated polyesters cure by a radical initiated polymerisation. They are mainly derived from reaction of an epoxy resin, e.g. bisphenol A diglycidyl ether, with acrylic or methacrylic acid. Their general formula is shown in Fig. 9.5, where R is any aliphatic or aromatic residue and R′ is typically either H or CH_3.

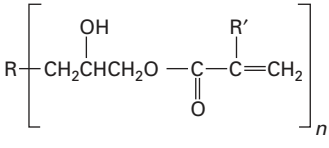

9.5

Like unsaturated polyesters they are copolymerised with diluents such as styrene using similar free radical initiators. They differ from polyesters in

that the unsaturation is at the end of the molecule and not along the polymer chain. When methacrylates are used, they offer better chemical resistance than unsaturated polyesters. Their burning behaviour falls between that of polyester and epoxy resins (LOI = 20–23).

Epoxy resins

These resins are extensively used in advanced structural composites particularly in the aerospace industry. They consist of an epoxy resin and a curing agent or hardener. They range from low-viscosity liquids to high melting point solids and can be easily formulated to give suitable products for the manufacture of prepregs by both the solution and hot-melt techniques. They can be easily modified with a variety of different materials. Epoxy resins are manufactured by the reaction of epichlorohydrin with materials such as phenols or aromatic amines. Epoxy resins contain the epoxy or glycidyl group shown in Fig. 9.6, where R is any aliphatic or aromatic residue.

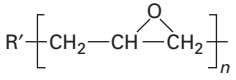

9.6

This group will react typically with phenolic —OH groups and Bisphenol-A type resins are most commonly used for composite structures. Epoxy resins are very reactive, hence both catalytic and reactive curing agents can be used. The general structure of a typical cured epoxy resin is shown in Fig. 9.7, where X can be H and Y depends upon the structure of curing agent.

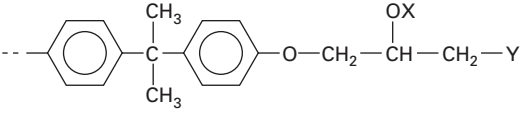

9.7

The resin can exist in the uncured state for quite a long time. This property allows the manufacture of prepregs, where the fibres are impregnated with resin and are partially cured [14]. Glass transition temperature of epoxies ranges from 120 to 220 °C [15], hence they can be safely used up to these temperatures. Apart from the simple example above, some of the epoxy resins used in advanced composites are *N*-glycidyl derivatives of 4,4′-diaminodiphenylmethane and 4-aminophenol, and aromatic di- and polyglycidyl derivatives of Bisphenol A, Bisphenol F, phenol novolacs and tris (4-hydroxyphenyl) methane [15].

Since the catalytic curing agents are not built into the thermoset structure, they do not affect the flammability of the resin. Reactive agents, mostly amines, anhydrides or phenolic resins, on the other hand, strongly affect the crosslinking of these thermosets and hence, their flammabilities [6]. Epoxy resins cured with amines and phenol–formaldehyde resins tend to produce more char than acid or anhydride-cured resin.

During the early stages of the thermal degradation (at lower temperatures) of cured epoxy resins, the reactions are mainly non-chain-scission type, whereas at higher temperatures, chain-scissions occur [16]. The most important non-scission reactions occurring in these resins are the competing dehydration and dehydrogenation reactions associated with secondary alcohol groups in the cured resin structures [16] (Fig. 9.8). The main products are methane, carbon dioxide, formaldehyde and hydrogen. Usually a large amount of methane is liberated before the start of scission reactions, which can be explained because of the reaction in Fig. 9.9.

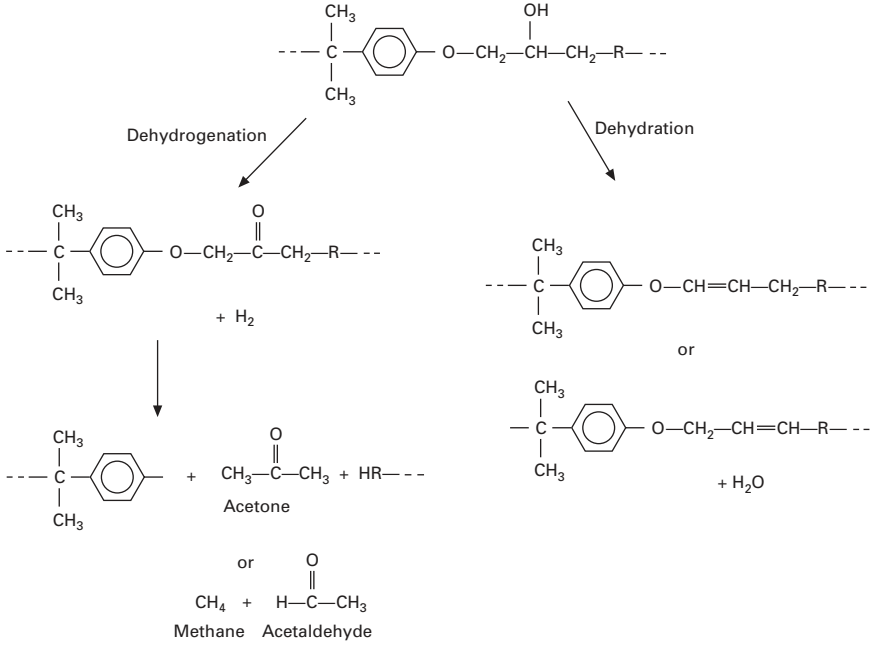

9.8

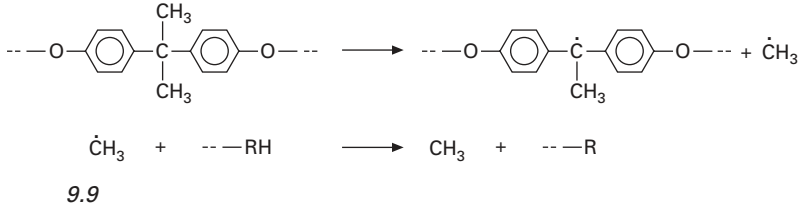

9.9

During chain-scission reactions the aliphatic segments break down into methane and ethylene (and possibly propylene) or acetone, acetaldehyde and methane (and probably carbon monoxide and formaldehyde) all of which are flammable (Fig. 9.10). From the aromatic segments of the polymer, phenol is liberated (Fig. 9.11).

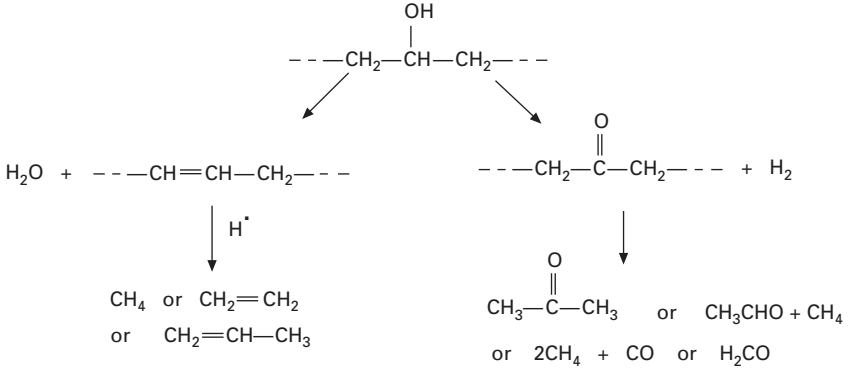

9.10

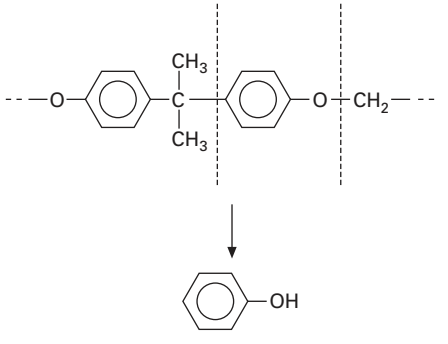

9.11

For phthalic anhydride-cured resins, phthalic anhydride is regenerated together with CO and CO_2. Other degradation products are benzene toluene, o- and *p*-cresols and higher phenols. In general, these are due to further break down or rearrangement of the aromatic segments of the resins. Phenols and cresols originate from Bisphenol A structural elements, whereas benzene, toluene, etc., originate from aromatic nuclei [16].

Aromatic amine-cured resins give large amounts of water in the temperature range 300–350 °C [17]. Thermal stability of aromatic-amine-cured epoxide resins depends on the aliphatic portion of the network [18]. The linkage present after curing (Fig. 9.12), differs from the glyceryl portion of bisphenol A-based epoxide in that the nitrogen replaces an oxygen atom (Fig. 9.13).

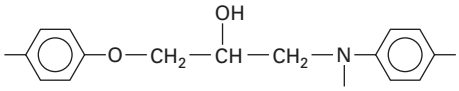

9.12

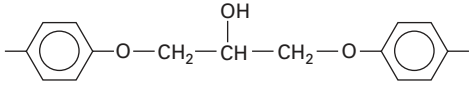

9.13

The flammable volatiles outlined above are, however, produced only in relatively small quantities and this, coupled with their crosslinked and related char-forming character, ensures that epoxy resins are less combustible than polyester resins with higher LOI values in the range 22–23. To confer acceptable levels of flame retardancy requires reactive flame retardants, such as tetrachloro- or tetrabromobisphenol-A and various halogenated epoxides which will act mainly as vapour-phase retardants to raise LOI values easily and significantly. Even the crosslinking agent may be flame retardant, as in the case of chlorendic anhydride, tetrabromo- or tetrachlorophthalic anhydride [19] or possibly phosphorus compounds [20]. Halogenated agents can be supplemented with antimony trioxide [13].

Additive flame retardants such as ammonium polyphosphate, tris (2-chloroethyl) phosphate or other phosphorus-containing plasticisers are also used. Alumina trihydrate used as a filler, is an effective flame retardant for epoxy resins [13].

Phenolic resins

Phenolic resins are manufactured from phenol and formaldehyde. Reaction of phenol with less than equimolar proportions of formaldehyde under acidic conditions gives so-called novolac resins containing aromatic phenol units linked predominantly by methylene bridges. Novolac resins are thermally stable and can be cured by crosslinking with formaldehyde donors such as hexamethylenetetramine. However, the most widely used phenolic resins for composites are resoles manufactured by reacting phenol with a greater than equimolar amount of formaldehyde under alkaline conditions. Resoles are essentially hydroxymethyl functional phenols or polynuclear phenols. Unlike novolacs, they are low-viscosity materials and are easier to process. Phenolic resins can also be prepared from other phenols such as cresols or bisphenols. The general formula is given in Fig. 9.14.

Phenolics are of particular interest in structural applications owing to their inherent fire-resistant properties yielding LOI values of 25 or so, although they tend to increase smoke generation. This high level of inherent flame

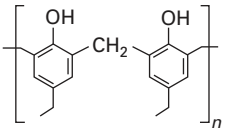

9.14

resistance often means that no further flame retarding is necessary to create composites having required performance levels. However, their main disadvantages are low toughness and a curing reaction that involves the generation of water. The water produced during curing can remain trapped within the composite and during a fire, steam can be generated, which can damage the structure of the material. This evolution is complemented by that generated chemically during the first step of thermal degradation [14], which may be because of phenol-phenol condensation by reactions of the type [10] shown in Fig. 9.15. The released water then helps in the oxidation of methylene groups to carbonyl linkages [6], which then decompose further, releasing CO, CO_2 and other volatile products to yield ultimately char (Fig. 9.16).

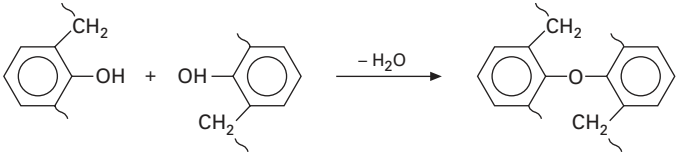

9.15

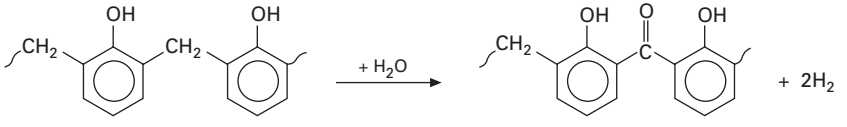

9.16

In the case of highly crosslinked material, water is not released until above 400 °C, and decomposition starts above 500 °C [10]. This was the case for all the phenolic resin samples examined by DTA, by ourselves and published elsewhere [21]. The amount of char depends upon the structure of phenol, initial crosslinks and tendency to crosslink during decomposition [12], and the main decomposition products are methane, acetone, carbon monoxide, propanol and propane.

Where phenolic resins require flame-retardant treatment, additive and reactive flame retardants can be used. Tetrabromobisphenol A, various organic phosphorus compounds, halogenated phenols and aldehydes (e.g. *p*-bromobenzaldehyde) are some of the reactive flame retardants used for phenolics.

Phosphorus can be introduced by direct reaction of the phenolic resin with phosphorus oxychloride. Likewise inorganic compounds such as boric acid may be incorporated into phenolic resin by chemical reaction [22].

Chlorine compounds (e.g. chloroparaffins) and various thermally stable aromatic bromine compounds may be utilised as additive flame retardant and antimony trioxide is usually added as a synergist. Suitable phosphorus compounds include halogenated phosphoric acid esters such as tris(2-chloroethyl) phosphate, halogenated organic polyphosphates, calcium and ammonium phosphates. Zinc and barium salts of boric acid and aluminium hydroxide also find frequent application [22]. In order to suppress the afterglow of phenolic resins, use is made of compounds such as aluminium chloride, antimony trioxide and organic amides.

Maleimide and polyimide resins

Thermosetting bismaleimide and polyimide resins are used widely in advanced composites. The general formula for polyimide resins is given in Fig. 9.17; their chemistry is often complex [15]. The processing conditions required to manufacture composite components from bismaleimide and other polyimide resins are more severe than used for epoxy systems and the resulting composites are more brittle than those of epoxy matrices. They cure at about 250–350 °C for several hours [15]. However, the glass transition temperature of cured resin is about 100 °C higher than cured epoxy matrices and hence they better retain mechanical properties at higher temperatures.

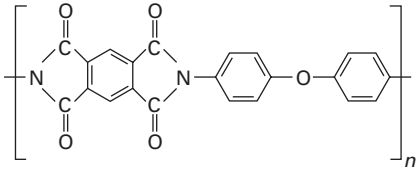

9.17

The aromatic structure of polyimides in particular ensures that they are characterised by high char formation on pyrolysis, low flammability (LOI > 30) and low smoke production when subjected to a flame in a non-vitiated atmosphere. Because of their high cost, they are only used in composites requiring the highest levels of heat and flame resistance.

Thermoplastic resins

Thermoplastic resins are high-molecular weight linear chain molecules with no functional side groups. They are fundamentally different from the thermosets

in that they do not undergo irreversible crosslinking reactions but instead melt and flow on application of heat and pressure and resolidify on cooling. However, to give composites with reasonable levels of physical heat resistance, their softening (or glass) transitions must be relatively high, which also influences cost of processing. For this reason, the more common thermoplastics such as polypropylene, polyamides 6 and 6.6 and the poly(alkylene terephthalates) are rarely used when heat and especially fire resistance are required. Some commonly used thermoplastic resins are poly(phenylene sulphide), poly(etheretherketone), poly(etherketone), poly(sulphone), poly(ether imide), poly(phenyl sulphone), poly(ether sulphone), poly(amide imide) and poly(imide). Their glass transition temperatures are 85, 143, 165, 190, 216, 220, 230, 249–288 and 256 °C, respectively [23]. All these resins have aromatic structures and so generally will be inherently flame resistant and have LOI values of at least 30, as shown in Table 9.2.

In a fire, such materials can soften enough to flow under their own weight and drip or run. The extent of dripping depends upon thermal environment, polymer structure, molecular weight, presence of additives, fillers, etc. Dripping can increase or decrease the fire hazard depending upon the fire situation. With small ignition sources, removal of heat and flame by the dripping away of burning polymer can protect the rest of material from spreading of the flame. In other situations, the flaming molten polymer might flow and ignite other materials.

Since thermoplastics are rarely used for rigid composites where the demands of both heat and fire resistance are paramount, the methods to impart flame retardancy are not discussed here. For further details regarding flame retardants for thermoplastic polymers, the reader should consult Kandola and Horrocks [1] and Horrocks [5] and cited references therein.

Resin–matrix interface

The fibre–matrix interface is an important region, which is required to provide adequate chemically and physically stable bonding between the fibres and the matrix. For example, aminosilane is used to bond glass fibre with epoxy matrix systems. Carbon fibre is both surface-treated in order to improve the mechanical properties of the composite, and coated with a sizing agent in order to aid processing of the fibre. Surface treatment creates potentially reactive groups such as hydroxyl and carboxyl groups upon the surface of the fibres, which are capable of reaction with the matrix. Epoxy-based sizing agents are quite common; however, they may not be suitable for the resin matrix [15].

The nature of the interface will affect the burning of the material as well. If the binding material is highly flammable, it will increase the fire hazard of the whole structure. However, if the interface is weak and two phases (fibre

and matrix) are pushed apart in case of fire, the matrix will burn more vigorously and inorganic fibres can no longer act as insulators. This situation is typical of layered textiles within a composite where delamination in fires will not only cause increased burning rates but also increase the rate of loss of mechanical properties and hence general product coherence. The use of interlinked reinforcing layers via use of 3D or stitched woven structures, for example, probably yields improved fire behaviour of the resulting composites although no work has been published in this area.

9.3 Flammability of composite structures

As discussed above, composite structures contain two polymeric structures, fibre and resin. Both of these polymeric components in a fire behave differently depending upon their respective thermal stabilities. Composite structures are often layered and thus tend to burn in layers. When heated, the resin of first layer degrades and combustible products formed are ignited. The heat penetrates the adjacent fibre layer and if inorganic fibre is used, it will melt or soften, whereas if organic fibre is used, it will degrade into smaller products depending upon its thermal stability. Heat then penetrates further into the underlying resin, causing its degradation and products formed will then move to the burning zone through the fibrous and, in some cases, resin chars. This will slow the burning front although if the structure is multilayered, it will burn in distinct stages as the heat penetrates subsequent layers and degradation products move to the burning zone through the fibrous layers. In general, the composite thickness of a structure can affect the surface flammability characteristics down to a certain limiting value. At this condition, where it is assumed that the composite has the same temperature through this limiting thickness, the material is said to be 'thermally thin'. However, above this depth, the temperature will be less than at the front face and a temperature gradient will exist where the material is not involved in the early stages of burning; here is said to be 'thermally thick' [24]. The transition from thermally thin to thermally thick is not a constant since it depends on material thermal properties including fibre and resin thermal conductivities.

For a given composite of defined thickness, the condition depends on the intensity of the fire or more correctly, the incident heat flux. While many large scale fire tests involve heat sources or 'simulated fires' having constant and defined fluxes, in real fires, heat fluxes may vary. For example, a domestic room filled with burning furniture at the point of flashover presents a heat flux of about 50 kW/m^2 to the containing wall and door surfaces; larger building fires present fluxes as high as 100 kW/m^2 and hydrocarbon fuel 'pool fires' may exceed 150 kW/m^2. We may examine the heat flux dependence on burning behaviour using calorimetric techniques such as the cone calorimeter [25]. For example, Scudamore [26] has shown by cone calorimetric analysis

that the thermally thin to thick effect for glass reinforced polyester, epoxy and phenolic laminates decreases as the external heat flux increases. Generally at heat fluxes of 35 and 50 kW/m^2, thin samples (3 mm) ignited easily compared with thick samples (9.5 mm), but at 75 and 100 kW/m^2 there was not much difference and all samples behaved as if they were 'thermally thin'.

The overall burning behaviour of a composite will be the sum of its component fibres and resin plus any positive (synergistic) or negative (antagonistic) interactive effects. Table 9.1 shows that as measured by limiting oxygen index, most commonly used fibres add little to the fuel content of a composite unless comprising fibres such as UHMW polyethylene or para-aramid. Table 9.2 presents results published in our previous review to illustrate the differences in fundamental component resin burning behaviour [1]. This table also demonstrates that in composites containing a non-flammable fibre reinforcing element such as glass, overall burning performance in terms of LOI reflects that of the resin although clearly, the glass component does have a fire retarding and hence LOI-raising property. From this and a number of studies and reviews [7–9, 27, 28] it may be concluded that ranking of fire resistance of thermoset resin composite components is:

> Phenolic > Polyimide > Bismaleimide > Epoxy
> > Polyester and vinyl ester

The superior performance of phenolics has been demonstrated above mechanistically in terms of their char-forming ability, which enables composites comprising them to retain mechanical strength for long times under fire conditions [29]. In addition, it is observed that because such composites encapsulate themselves in char, they do not produce much smoke [30]. Epoxy and unsaturated polyesters on the other hand carbonise less than phenolics and as demonstrated above, produce more fuels during pyrolysis and so continue to burn in a fire. Furthermore, those containing aromatic structures such as styrenic moieties produce more smoke. However, while phenolics have inherent flame-retardant properties, their mechanical properties are inferior to other thermoset polymers, such as polyester, vinyl ester and epoxies [29]. Hence, they are less favourable for use in load-bearing structures. Epoxies on the other hand, because of very high mechanical strength, are the more popular choice.

Char formation is the key to achieving low flammability and good fire performance. This is because char is formed at the expense of possible flammable fuel formation (contrast the flammable volatiles formed during polyester and epoxy resin thermal degradation in the previously shown mechanisms with the char-forming tendency of phenolics). In addition, because char 'locks in' the available carbon, less smoke can be formed and the char acts as a barrier to its release should it be formed. Furthermore, the char acts as an insulating layer and protects the underlying composite structure and

this also helps to minimise the loss in tensile properties during fire exposure. In other words there is a direct relationship between flammability of a polymer and its char yield as discussed comprehensively by van Krevelen [30]. Gilwee *et al.* [31] and Kourtides [32] have found that a linear relationship exists between limiting oxygen index and char yields for resins and graphite reinforced composites respectively as shown in Fig. 9.18. This shows that composite structures behave similarly to bulk resin polymers, that char formation determines the flammability of the composite and that the presence of inorganic fibre does not improve the flame retardancy of the structure.

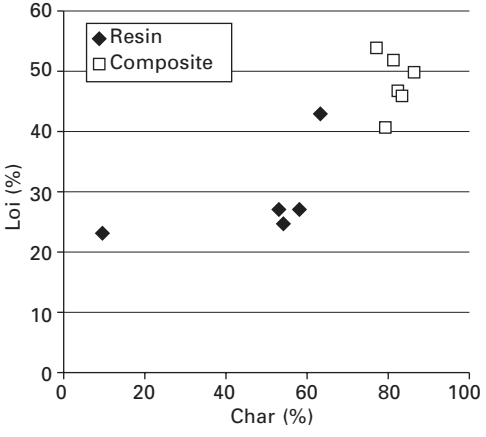

9.18 Plot of LOI versus char formation for a series of resins and graphite fabric (8-harness satin weave) reinforced composites [31, 32].

Brown *et al.* [33] have studied the fire performance of extended-chain polyethylene (ECPE) and aramid fibre-reinforced composites containing epoxy, vinyl ester and phenolic matrix resins by cone calorimetry. Various parameters were determined for ECPE and aramid fabrics only, matrix resins only and their composites and maximum or peak heat release rates (PHRR) only are plotted in (Fig. 9.19). ECPE reduced the flammability of epoxy but increased it for vinyl ester matrix resins. Aramid, on the other hand, had little effect on time to ignition (compared with resin alone) except for the phenolic, but reduced RHR. In general, resin and reinforcement contributions to the composite rate of heat release behaviour as a function of time are discernible and depend on respective flame-retardant mechanisms operating and levels of their transferability and possible synergisms and antagonisms. This indicates that a flame or heat-resistant fibre can be effective for one type of resin but not necessarily for another.

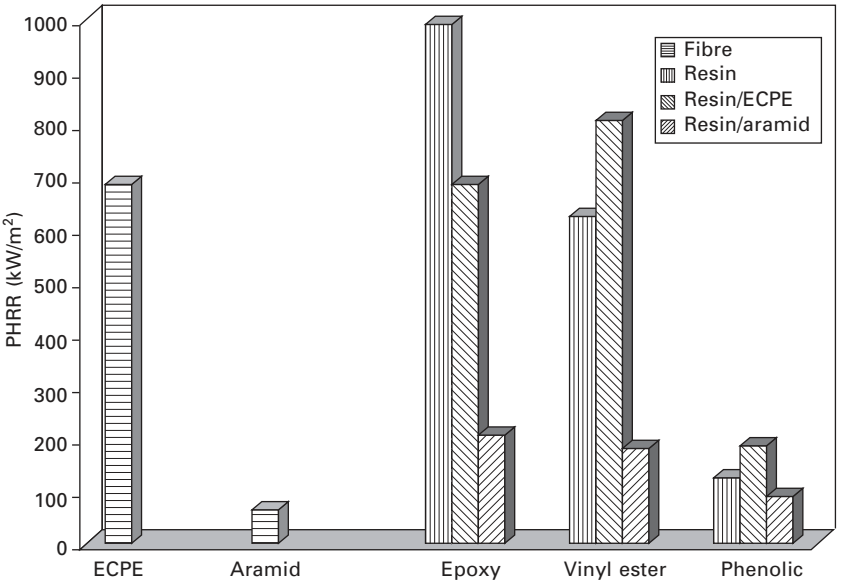

9.19 Maximun or peak, PHRR values for fibre reinforcements, matrix resins and composite materials at 50 kW/m^2 cone irradiance [33].

9.4 Methods of imparting flame retardancy to composites

As composites continue to replace more conventional materials, their fire performance is increasingly being questioned, especially the poor smoke-generating character of polyester-resinated composites that constitute the majority of the present world market. Unfortunately, imparting flame retardancy and smoke reduction to composites often results in reductions of their mechanical strengths. Therefore, achieving a certain level of flame retardancy while maintaining other such properties is a major challenge. Following our recently published reviews [1, 3] of the work done in this field where we discuss the more basic means of conferring flame retardancy, here we extend these studies to include research work undertaken in our own and other laboratories since 1999.

9.4.1 Use of inherently flame-resistant resins and/or fibres

The reinforcing fibre phase can be rendered flame retardant by appropriate treatment or by the use of high heat and flame-resistant fibres [34], such as aramids or carbon as shown in Table 9.1, although the flame retardancy levels desired should really match those of the matrix if high levels of fire performance are to be realised. Hshieh and Beeson [35] have tested flame-

retarded epoxy (brominated epoxy resin) and phenolic composites containing fibre glass, para-aramid (e.g. Kevlar®, Du Pont) and graphite fibre reinforcements using the NASA upward flame test and the controlled atmosphere, cone-calorimeter test. The upward flame propagation test showed that phenolic/graphite had the highest and epoxy/graphite composites had the lowest flame resistance as shown in Fig. 9.20. This is an interesting case that shows that the overall fire performance is not simply the average of the components present. The most flame-resistant graphite or carbon reinforcement has produced the most flammable composite with epoxy possibly because the carbon fibres prevent the liquid decomposition products from the resin from dripping away in the upward flame test – this so-called 'scaffolding effect' is seen in blends of thermoplastic and non-thermoplastic fibres in textiles [5]. Conversely, the presence of the char-forming phenolic will complement the carbon presence in the graphite reinforcement and so present an enhanced carbon shield to the flame. Controlled-atmosphere cone calorimetry also showed that phenolic composites had lower values of time of ignition, peak heat release rate, propensity to flashover and smoke production rate.

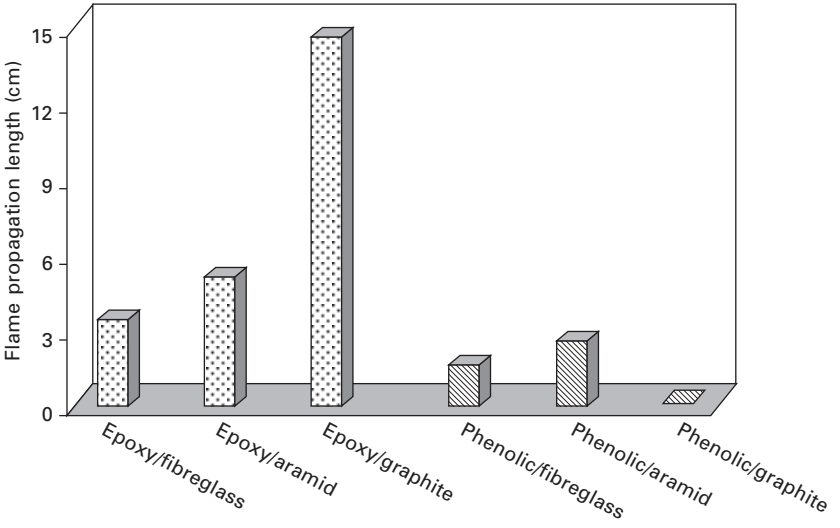

9.20 Flame propagation lengths of composites [35].

9.4.2 Chemical or physical modifications of resin matrix

Conventional flame retardants

Additives such as zinc borate and antimony oxide have been used with halogenated polyester, vinyl ester or epoxy resins [29, 36]. Alumina trihydrate

(ATH) and bromine compounds are other examples [37]. However, many of these resins and additives are ecologically undesirable and in a fire increase the amount of smoke and toxic fumes given off by the burning material. Furthermore, of all methods of improving fire resistance, this usually results in a reduction in the mechanical properties of the composite structure.

Scudamore [26] has studied the effect of flame retardants on the fire performance of glass-reinforced polyester, epoxy and phenolic laminates by cone calorimetry. The polyester laminates examined comprised a brominated resin whereas fibre reinforced (FR) epoxy and phenolic resins contained ATH. ATH was used in the FR phenolic laminate. While generally it was concluded that the fire properties depend on the type of resin and flame retardant, the type of glass reinforcement and for thin laminates, the thickness, more specifically, flame retardants for all resins delay ignition and decrease heat release rates. Again, phenolic laminates showed lower flammability than either FR polyester or epoxy resins and addition of ATH further enhanced flame retardancy by reducing maximum or peak rate of heat release rate values values to less than 100 kW/m^2 at 50 kW/m^2 heat flux.

Morchat and Hiltz [38] and Morchat [39] have studied the effect of the FR additives antimony trioxide, alumina trihydrate and zinc borate on the flammability of flame-retardant polyester, vinyl ester and epoxy resins by thermogravimetric analysis (TGA), smoke production, toxic gas evolution, flame spread and oxygen index methods. Except for epoxy resin, the others contained halogenated materials from which they derived their fire-retardancy characteristics through the vapour phase activity of chlorine and/or bromine. In most cases, with a few exceptions, the additives lowered the rate of flame spread (by 2–70%), increased LOI (by 3–57%) and lowered specific smoke optical density (by 20–85%), depending on the fire retardant and the resin system evaluated. However, for the majority of resins, the addition of antimony trioxide resulted in an increase in smoke production. The best performance was observed upon addition of zinc borate to the epoxy resin.

Nir *et al*. [40] have studied the mechanical properties of brominated flame retarded and non-brominated epoxy (tris-(hydroxyphenyl)-methane triglycidyl ester)/graphite composites. While the incorporation of bromine did not change the mechanical properties within ±10% of those of the non-brominated resin, it helped in decreasing water absorption and increasing environmental stability, thereby indicating that this is an easy method to flame retard without unduly influencing the impact strength of graphite-reinforced composites.

Intumescents

In our earlier review, we considered the potential for inclusion of intumescents within the composite structure and noted at that time (1998), very little interest had been shown [3]. Kovlar and Bullock [41] have reported using an

intumescent component as an additive in a phenolic matrix and developed a formulation with phenolic resin and intumescent in 1:1 ratio, reinforced with glass fabric. Upon exposure to fire the intumescent composite panel immediately began to inflate, foam, swell and char on the side facing the fire, forming a tough, insulating, fabric-reinforced carbonaceous char that blocked the spread of fire and insulated adjacent areas from the intense heat. These intumescent-containing samples showed marked improvement in the insulating properties than control phenolic or aluminium panels.

Most work since that time has been undertaken in our own laboratories based on a patent awarded in 1995 [42] in which novel combinations of intumescent and flame-retardant fibres are described. These yield complex 'char-bonding' structures when heated, which demonstrate unusually high fire and heat resistance compared with individual component performance. Work at the University of Bolton since 1998 has extended this concept into composite structures where the flame-retardant fibre component may become part of the reinforcement and the FR fibre-intumescent system interacts positively with the otherwise flammable resin component present. From this work, a number of publications and a second patent have arisen [21, 43–49].

We have studied the possible interaction between resin (polyester, epoxy and phenolic) with a phosphate-based intumescent and FR cellulosic fibre (Visil, Sateri) with thermal analytical techniques [21]. Studies of different components and their mixtures in different combinations indicated that, on heating, all components degrade by physically and chemically compatible mechanisms, resulting in interaction and enhanced char formation. This led to the preparation of composite laminates, where these components were added either as additives in pulverised form or fibre interdispersed with intumescent as a fabric scrim for partial replacement of glass fibre [46, 47]. The composite series in Table 9.3 were prepared to investigate the effect of thickness and nature of glass reinforcement (random matt versus woven) (PS1–PS6) for polyester resin-based composites. A similar set of epoxy-based composites, EP1–EP3 also comprising combinations of intumescent and FR celluosic were fabricated. The intumescent comprised melamine phosphate and glass fabrics were typically 300 g/m^2

LOI results for polyester sample PS1–PS3 are only slightly increased with intumescent presence (PS2, 22.6%) and is unaffected by additional presence of Visil (PS3, LOI = 22.6%) and these suggest that the composites will still burn in air in spite of the intumescent (Int) and FR viscose (Vis) presence. However, for epoxy composites, the presence of intumescent raises LOI from 27.5 (EP1) to 35.2% (EP2) and with additional Visil, to 36.2% (EP3), in both cases composites will not ignite and sustain burning in air.

Cone calorimetry (under 50 kW/m^2 external heat flux) behaviour is typified by the heat release rate (HRR) properties shown in Figs 9.21 and 9.22. Generally, the addition of intumescent and/or FR viscose has little effect on

Table 9.3 Physical and LOI properties of composite laminates [46, 47]

Sample No.	Sample details	Mass fraction (%)				Thickness (mm)	LOI (%)
		Glass	Resin	Visil	Intumescent		
Polyester (PS) laminates with four layers of random mat glass							
PS 1	Res	39.9	60.1	–	–	2.7	19.3
PS 2	Res + Int	29.5	64.2	–	6.3	3.8	22.6
PS 3	Res + Vis + Int	25.8	62.0	6.1	6.1	4.6	22.6
Polyester (PS) laminates with four layers of woven roving glass*							
PS 4	Res	62.7	37.3	–	–	1.0	–
PS 5	Res + Int	57.2	38.8	–	3.8	1.2	–
PS 6	Res + Vis + Int	49.6	42.2	4.1	4.1	1.5	–
Epoxy laminates with four layers of woven roving glass*							
EP 1	Res	55.0	45.0	–	–	1.9	27.5
EP 2	Res + Int	53.0	42.3	–	4.7	2.0	35.2
EP 3	Res + Vis + Int	50.0	40.0	5.0	5.0	2.3	36.2

Note: *Woven roving glass fabrics used here have plain weave structures.

the time to ignition and extinction times, but does reduce the peak heat release rate values, which in a real fire, is the measure of the ability of a fire to grow in intensity. For polyester-based composites PS1–PS3, Fig. 9.21(a) shows this effect for samples of increasing thickness and hence fuel load and PHRRs decrease from 314 to 246 kW/m^2. Where composite thickness is almost constant, however, the effects of intumescent and intumescent-treated FR viscose fabric are less with peak heat release values reducing from 477 to 387 kW/m^2 (see Fig. 9.21b). These effects are particularly noticeable in the epoxy-based composites (see Fig. 9.21c) where PHRR values reduce from 385 to 262 kW/m^2, reflecting behaviour of LOI results.

Since the char retained after burning a polymer is also a measure of its flammability, the mass loss curves accompanying heat release data give insight into the fire performance of the samples. For polyester samples PS1–PS3, mass loss curves as a function of time and for all samples the effect of additives on the residual char retained after 300 s (360 s for samples PS1–PS3) are given in Fig. 9.22. Figure 9.22(a) shows that presence of intumescent (sample PS2) and Visil-intumescent (sample PS3) makes the samples more thermally stable than resin only (PS1) for about 240 s by slowing down volatilisation and burning. But after complete combustion, residual chars for these samples are less than control sample as can be seen from Fig. 9.22(b).

Mass loss curves for epoxy samples showed that the presence of intumescent alone and with Visil fibre increases the residual mass at any time [47] and even after complete combustion after about 300 s, as can be seen from Fig. 9.22(b). This supports our earlier thermal analytical results [21] that these components promote char formation of the resin.

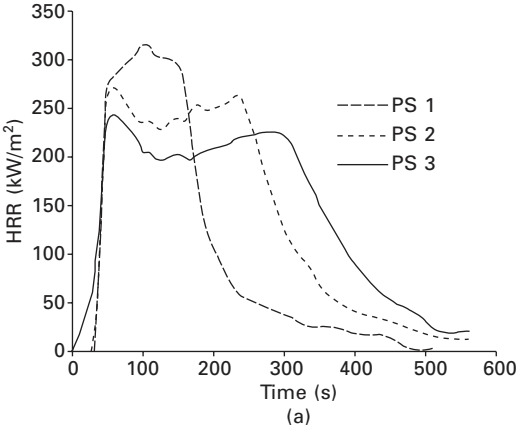

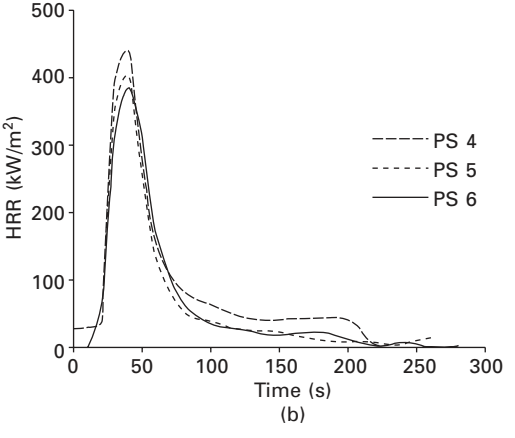

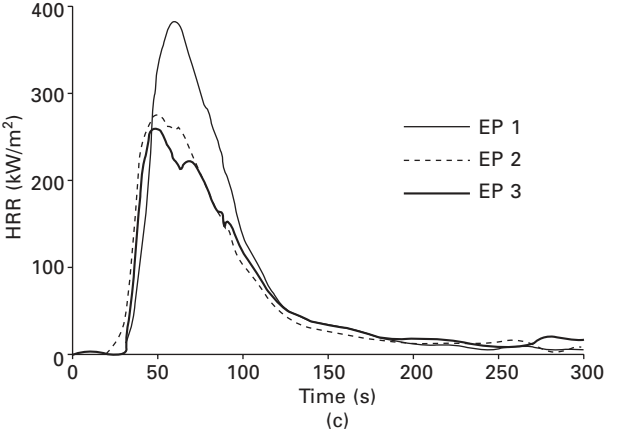

9.21 HRR versus time curves of (a), (b) polyester and (c) epoxy composite laminates at 50 kW/m^2 heat flux.

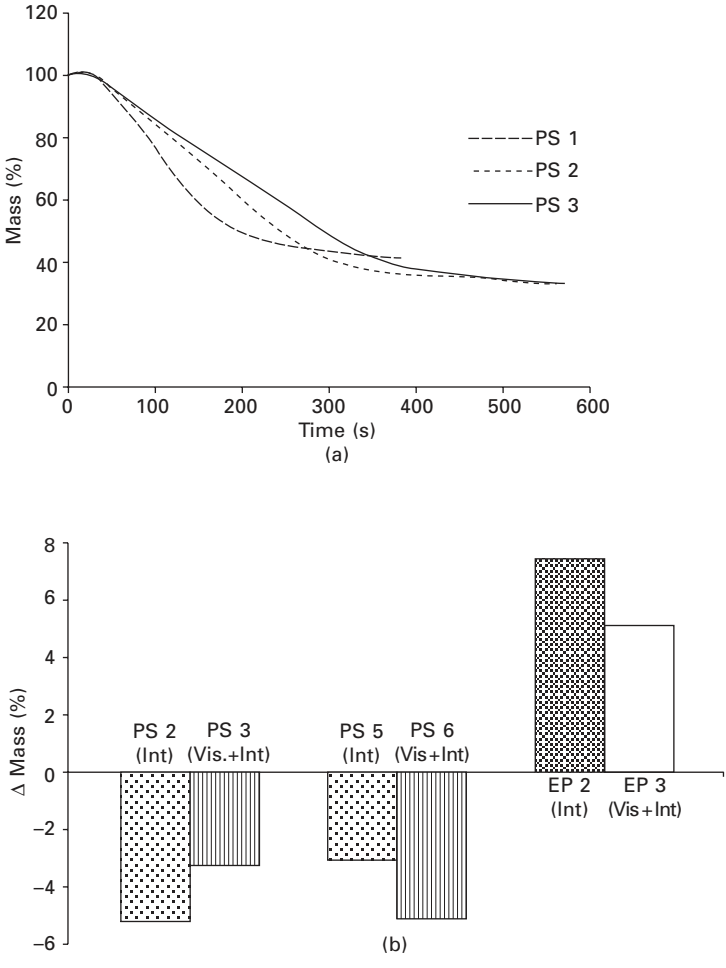

9.22 (a) Mass loss versus time curves of PS1-PS3 samples at 50 kW/m^2 heat flux and (b) change in residual mass (Δ mass%) of PS2, PS3, PS5, PS6, EP2, EP3 samples compared with respective control PS1, PS4 and EP1 samples.

Smoke production appears to increase from PS1 to PS3 measured during cone calorimetry, although when measured using the standard 'NBS Smoke Chamber' according to ASTM E662, a reduction is seen [45]. However, for epoxy resin-based samples, a progressive decrease in smoke generation is seen for EP1, 2 and 3 samples. These results again illustrate the apparent synergy between the intumescent system and the epoxy resin matrix.

The charred epoxy samples EP1–EP3 left from cone-calorimetric tests were examined for changes in appearance by taking photographs with a digital camera. These samples were also examined under an optical microscope

for finer details on the surface and through cross-sections of the laminates. Results are shown in Figs 9.23 and 9.24; in the latter, cross-sectional micrographs show evidence of delamination.

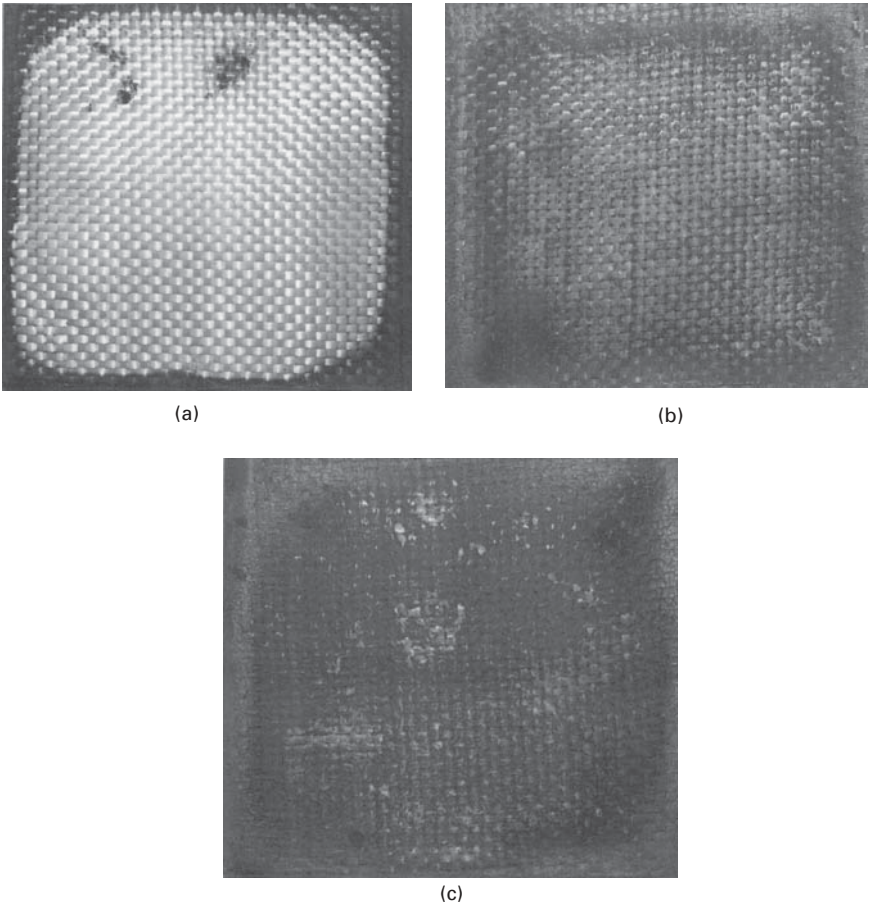

9.23 Images with a digital camera of samples (a) EP1 (b) EP2 and (c) EP3 after cone experiments.

Figure 9.23(a) for the control sample (EP1), which contains glass fibre and resin only, shows that after cone exposure all the resin has burned away. Charred residue on the edges is due to the shielding effect of the sample holder edge during the cone experiments. The cross-sectional view in Fig. 9.24(a) also shows that most of the resin has burned and only glass fibre is seen in the first five layers. The effect of intumescent additive (sample EP2) on the burning behaviour of resin is clearly seen in Fig. 9.23(b), where charred residues are seen on the surface and within layers of glass fabric in

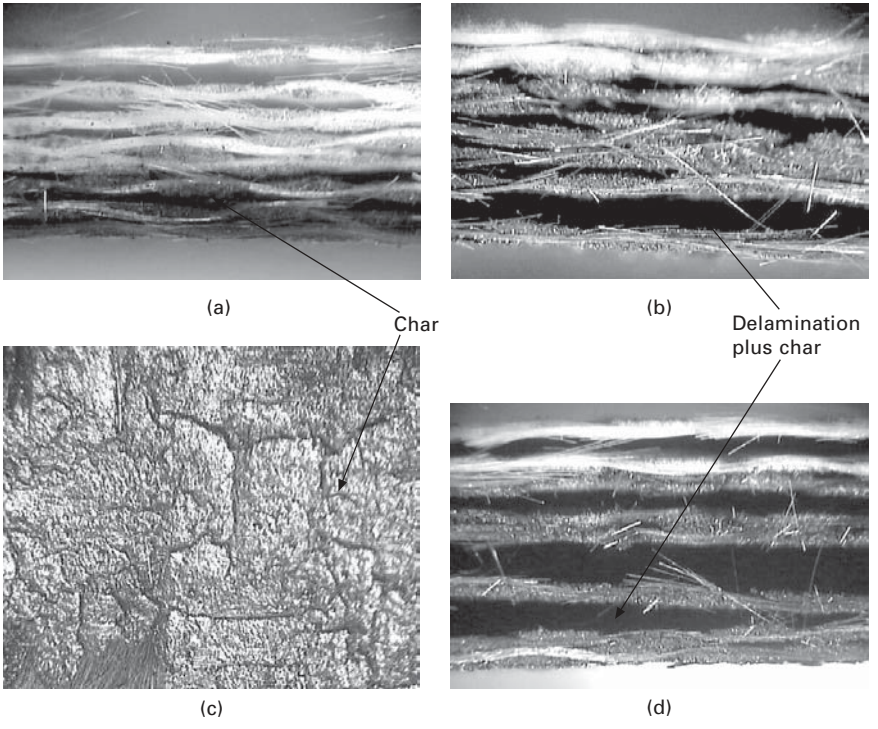

9.24 Optical microscopic images of samples EP1–EP3 after cone experiment.

cross-sectional view (Fig. 9.24b). However, when both Visil and intumescent are present as additives (sample EP3), the char formed is higher in quantity as seen on the surface (Fig. 9.23c and 9.24c) and between layers of glass fibre (Fig. 9.24d). The char on the surface of sample EP3, when seen under the microscope, shows the complexity of the charred structure, the chemical nature of which has been discussed in detail elsewhere [21].

9.4.3 Use of external coatings and outer protective surfaces

Another way of flame-retarding or fire-hardening composite structures is to use flame-retardant (usually intumescent based) paints or coatings. Intumescent systems are chemical systems, which by the action of heat evolve gases and form a foamed char. This char then acts as an insulative barrier to the underlying structural material against flame and heat. One very effective intumescent coating is fluorocarbon latex paint [50].

Tewarson and Macaione [51] have evaluated the flammability of glass/resin composite samples treated with intumescent and ceramic coatings by

FMRC (Factory Mutual Research Corporation) 50 kW-scale apparatus (discussed in ref. 51) methods. As expected, the calculated thermal response parameter (TRP) values showed that ceramic and intumescent coatings are quite effective in improving fire resistance. The intumescent coatings were superior on the vinyl ester and phenolic resinated composites while the ceramic coating was best on the epoxy composite.

Sorathia *et al.* [52] have explored the use of integral, hybrid thermal barriers to protect the core of the otherwise flammable composite structure. These barriers function as insulators and reflect the radiant heat back towards the heat source, which delays the heat-up rate and reduces the overall temperature on the reverse side of the substrate. Treatments evaluated included ceramic fabrics, ceramic coatings, intumescent coatings, hybrids of ceramic and intumescent coatings, silicone foams and a phenolic skin. The composite systems evaluated in combination with thermal barrier treatments included glass/vinyl ester, graphite/epoxy, graphite/bismaleimide and graphite/phenolic combinations. All systems were tested for flammability characteristics by cone-calorimetry and PHRR values at 75 kW/m^2 cone irradiance are plotted in Fig. 9.25. Without any barrier treatment, all composites failed to meet the ignitability and PHRR requirements, whereas all treated ones passed. Ceramic/intumescent hybrid coatings seem to be very effective. More recently Sorathia *et al.* have conducted an investigation of different commercial protective intumescent coatings for potential use on ships for the US Navy [53]. All coatings failed the fire performance criteria necessary to meet the US Navy requirements for high-temperature fire insulation in accordance with draft

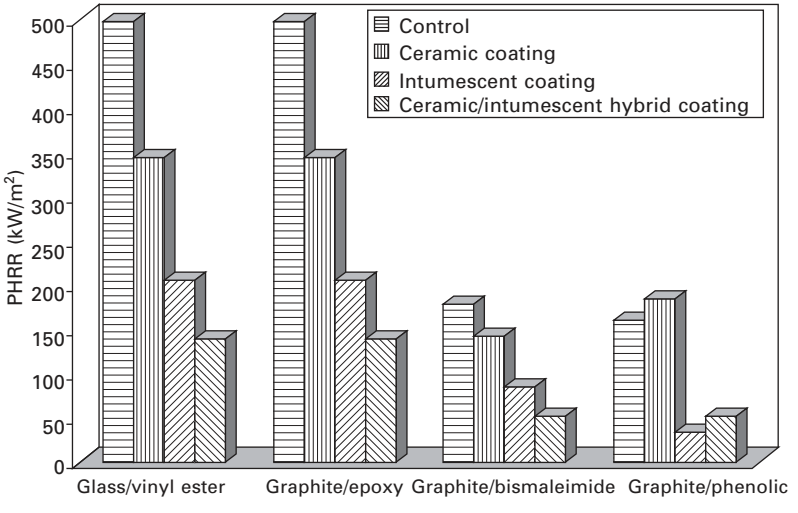

9.25 Peak heat release rate (PHRR) values for composite materials with thermal barrier treatment at 75 kW/m^2 cone irradiance [52].

military standard DRAFT MIL_PRF_XX 381. This led them to conclude that intumescent coatings are not sufficient to protect shipboard spacings during a fire and are not equivalent when used alone as direct replacement for batt or blanket-type fibrous fire insulation (e.g. mineral wool, StrutoGard®) installed aboard ships. However, some of these coatings, when used combined with blanket-type fibrous fire insulation, were effective in meeting fire resistance criteria.

While the use of mineral and ceramic claddings is quite popular for naval applications [41] in preference to flameproof conventional composite hull, deck and bulkhead structures, the main disadvantages are that they occupy space, add significant weight and can act as an absorbent for spilled fuel or flammable liquid during a fire. When this occurs, extinguishing the fire will be more difficult and the insulating property of the ceramic wool is lost. However, if the mineral cladding as a fibrous membrane is incorporated as the final layer within the composite structure then this last problem is overcome and a 'fire hardened' face may be introduced to the otherwise flammable core. Such a system overlaps with the intumescent developments made in our own laboratories [43–48] as well as those developed by Sorathia [52, 53].

One recent UK commercial example of this sort of product is the Technofire® range of ceramic wet-laid, nonwoven webs produced by Technical Fibres Ltd in the UK; these are available with a number of different inorganic fibres, including glass and rock wool either with or without an associated exfoliated graphite present. They are designed to be compatible with whatever resin is used in composite production.

9.5 Conclusions

Fire performance of fibre reinforced composites is becoming increasingly important not only as composite usage increases generally, but also as regulations in construction and transport sectors, especially, become more stringent in regard of increased fire safety. Within military circles, composites are replacing metals in traditional naval and armoured vehicle applications where fire performance is as important as mechanical and ballistic properties. From the above discussion it can be concluded that choices of resin and fibre are crucial in determining the flammability properties of the whole structure. Because resins make up a significant fraction of all composites and these are organic in character, then they are the prime sources of fuel when composites are heated. We have demonstrated that relative fuel-generating tendencies are wholly dependent upon respective resin chemistries and that the presence of inorganic fibres such as glass and carbon does not help in reducing overall flammability. If flame-retardant chemicals, which are compatible with both fibres and resin matrix, are selected, resulting effects can be synergistic both

towards improved fire performance but also positively or negatively towards smoke suppression. Within the most common composite markets where the cheaper and more flammable polyester resins are used, smoke generation, already large, and its consequent suppression is an equally significant fire performance factor; it is here that the traditional antimony–bromine formulations are weak and considerable interest lies in finding alternatives with comparable flame-retarding properties but with enhanced smoke reduction. Use of intumescents and the work in our own laboratories has shown encouraging results to date and confirms that char-forming agents are the best way forward. The role of nanoclays and nanocomposite structures within the macrocomposite itself is currently being addressed by a number of research teams, including our own. The next few years promise much excitement in the discovery of novel fire-resistant systems that will have superior performance to present systems and will be based on both present and developing fire science understanding.

9.6 References

1. Kandola B.K. and Horrocks., 'Composites' in Horrocks A.R. and Price D. (Eds), *Fire Retardant Materials*, Cambridge, Woodhead Publishing, 2001.
2. Jones F.R., 'Glass Fibres', in Hearle J.W.S. (Ed), *High-performance Fibres*, Cambridge, Woodhead Publishing, Chapter 2, 2001.
3. Kandola B.K. and Horrocks A.R., 'Flame retardant composites, a review : the potential for use of intumescents', in Bras M.L., Camino G., Bourbigot S. and Delobel R. (Eds), *Fire Retardancy of Polymers – The Use of Intumescence*, Cambridge, The Royal Society of Chemistry, 1998.
4. *Toxicological Risks of Selected Flame-Retardant Chemicals*, Sub-committee on Flame-retardant Chemicals of the United States National Research Council, Washington, DC; National Academy Press, Washington, 2000.
5. Horrocks A.R., 'Textiles' in Horrocks A.R. and Price D., (Eds), *Fire Retardant Materials*, Cambridge, Woodhead Publishing, Chapter 4, p. 128, 2001.
6. Levchik S.V., 'Thermosetting Polymers', in Bourbigot S., Le Bras M., Troitzsch J. (Eds), *Fundamentals in International Plastics Flammability Handbook*, 3rd edition, in press.
7. Brown J.E., Loftus J.J. and Dipert R.A., *Fire Characteristics of Composite Materials – A Review of the Literature*, Report 1986, NBSIR 85-3226.
8. Kourtides D.A. *et al*., 'Thermochemical characterisation of some thermally stable thermoplastic and thermoset polymers', *Polym. Eng. Sci*., 1979, **19(1)**, 24–29.
9. Kourtides D.A., *et al*., 'Thermal response of composite panels', *Polym. Eng. Sci*., 1979, **19(3)**, 226–231.
10. *Fire Safety Aspects of Polymeric Materials, Vol 1 – Materials State of Art*, Chapter 6, A Report by National Materials Advisory Board, National Academy of Sciences, Technomic Publ. Washington, 1977.
11. Learmonth G.S. and Nesbit A., 'Flammability of polymers V. TVA (Thermal volatilization) analysis of polyester resin compositions', *Br. Polym. J*., 1972, **4**, 317.

12. Das A.N. and Baijaj S.K., 'Degradation mechanism of styrene–polyester copolymer', *J. Appl. Polym. Sci*., 1982, **27**, 211.
13. Pal G. and Macskasy H., *Plastics – Their Behaviour in Fires*, Chapter 5, Amsterdam, Elsevier, 1991.
14. Vasiliev V.V., Jones R.M. and Man L.I. (Eds), *Mechanics of Composite Structures*, Washington, Taylor and Francis, 1988.
15. Phillips L.N. (Ed), *Design with Advanced Composite Materials*, London, Springer-Verlag, 1989.
16. Bishop D.P. and Smith D.A., 'Combined pyrolysis and radiochemical gas chromatography for studying the thermal degradation of epoxy resins and polyimides. I. The degradation of epoxy resins in nitrogen between 400° and 700 °C', *J. Appl. Polym. Sci*., 1970, **14**, 205.
17. Paterson-Jones J.C., 'The mechanism of the thermal degradation of aromatic amine-cured glycidyl ether-type epoxide resins' *J. Appl. Polym. Sci*., 1975, **19**, 1539.
18. Paterson-Jones J.C., Percy V.A., Giles R.G.F. and Stephen A.M., 'The thermal degradation of model compounds of amine-cured epoxide resins' *J. Appl. Polym. Sci*., 1975, **17**, Part I, 1867–1876, Part II, 1877–1887.
19. Lo J. and Pearce E.M., 'Flame-retardant epoxy resins based on phthalide derivatives', *J. Polym. Sci. Polym. Chem. Ed*., 1984, **22**, 1707.
20. Mikroyannidis J.A. and Kourtides D.A., 'Fire resistant compositions of epoxy resins with phosphorus compounds', *Polym. Mat. Sci. Eng. Proc*., 1983, **49**, 606.
21. Kandola B.K., Horrocks A.R., Myler P. and Blair D., in Nelson G.L. and Wilkie C.A. (Eds), *Fire and Polymers*, ACS Symp. Ser., American Chemical Society, Washington, DC, 2001, 344.
22. Troitzsch J., *International Plastics Flammability Handbook*, Chapter 5, Munich, Hanser Publ., 1990.
23. Eckold G., *Design and Manufacture of Composite Structures*, Cambridge, Woodhead Publishing, 1994.
24. Mikkola E. and Wichman I.S., 'On the thermal ignition of combustible materials', *Fire Mater*., 1989, **14**, 87–96.
25. Babrauskas V. and Grayson S.J., *Heat Release in Fires*, London and New York, Elsevier Applied Science, 1992.
26. Scudamore M.J., 'Fire performance studies on glass-reinforced plastic laminates', *Fire Mater,* 1994, **18**, 313–325.
27. Brown J.E., Braun E. and Twilley W.H., *Cone Calorimetric Evaluation of the Flammability of Composite Materials*, Report 1988, NBSIR-88–3733.
28. Brown J.R. and St John N.A., 'Fire-retardant low-temperature-cured phenolic resins and composites', *TRIP,* 1996, **4(12)**, 416–420.
29. Gabrisch H.-J. and Lindenberger G., 'The use of thermoset composites in transportation: their behaviour', *SAMPE J*., 1993, **29(6)**, 23–27.
30. van Krevelen D.W., 'Some basic aspects of flame resistance of polymeric materials', *Polymer*, 1975, **16**, 615–620.
31. Gilwee W.J., Parker J.A. and Kourtides D.A., 'Oxygen index tests of thermosetting resins', *J. Fire Flamm*., 1980, **11(1)**, 22–31.
32. Kourtides D.A., 'Processing and flammability parameters of bismaleimide and some other thermally stable resin matrices for composites' *Polym. Compos*., 1984, **5(2)**, 143–150.
33. Brown J.R., Fawell P.D. and Mathys Z., 'Fire-hazard assessment of extended-chain polyethylene and aramid composites by cone calorimetry', *Fire Mater*., 1994, **18**, 167–172.

34. Horrocks A.R., Eichhorn H., Schwaenke, Saville N. and Thomas C., 'Thermally resistant fibres,' in Hearle J.W.S. (Ed), *High Performance Fibres*, Cambridge, Woodhead Publishing, Chapter 9, 2002.
35. Hshieh F.Y. and Beeson H.D., 'Flammability testing of flame-retarded epoxy composites and phenolic composites', *Proc. 21st Int. Conf. on Fire Safety*, San Francisio 1996, **21**, 189–205.
36. Stevart J.L., Griffin O.H., Gurdal Z., Warner G.A., 'Flammability and toxicity of composite materials for marine vehicles', *Naval Engn. J*., 1990, **102(5)**, 45–54.
37. Georlette P., 'Applications of halogen flame retardants' in Horrocks A.R. and Price D. (Eds), *Fire Retardant Materials*, Cambridge, Woodhead Publishing, Chapter 8, 2001.
38. Morchat R.M. and Hiltz J.A., 'Fire-safe composites for marine applications', *Proc 24th Int. SAMPE Tech. Conf.* Toronto, 1992, T153–T164.
39. Morchat R.M., *The Effects of Alumina Trihydrate on the Flammability Characteristics of Polyester, Vinylester and Epoxy Glass Reinforced Plastics*, Techn. Rep. Cit. Govt. Rep. Announce Index (US), 1992, **92(13)**, AB NO 235, 299.
40. Nir Z., Gilwee W.J., Kourtides D.A. and Parker J.A., 'Rubber-toughened polyfunctional epoxies: brominated vs nonbrominated formulated for graphite composites', *SAMPE Q*., 1983, **14(3)**, 34–38.
41. Kovlar P.F. and Bullock D.E., 'Multifunctional intumescent composite fire barriers' in Lewin M. (Eds), *Proc. of the 1993 Conf. Recent Advances in Flame Retardancy of Polymeric Materials*,Vol IV, BCC, Stamford, Conn., 1993, 87–98.
42. Horrocks A.R., Anand S.C. and Hill B., Fire and heat resistant materials. UK Pat. 2279084B, 21 June 1995.
43. Kandola B.K. and Horrocks A.R., 'Complex char formation in flame-retarded fibre-intumescent combinations – III Physical and chemical nature of the char', *Text. Res. J*.,1999, **69(5)**, 374–381.
44. Kandola B.K. and Horrocks A.R., 'Complex char formation in flame-retarded fibre-intumescent combinations – IV. Mass loss and thermal barrier properties', *Fire Mater*., 2000, **24**, 265–275.
45. Horrocks A.R., Myler P., Kandola B.K. and Blair D., Fire and heat resistant materials. Patent Application PCT/GB00/04703 December, 2000.
46. Kandola B.K., Horrocks A.R., Myler P. and Blair D., 'The effect of intumescents on the burning behaviour of polyester-resin-containing composites', *Composites Part A*, 2002, **33**, 805–817.
47. Kandola B.K., Horrocks A.R., Myler P. and Blair D., 'New developments in flame retardancy of glass-reinforced epoxy composites', *J. Appl. Polym. Sci*., 2003, **88(10)**, 2511–2521.
48. Kandola B.K., Horrocks A.R., Myler P. and Blair D., 'Mechanical performance of heat/fire damaged novel flame retardant glass – reinforced epoxy composites', *Composites Part A*, 2003, **34**, 863–873.
49. Neininger S.M., Staggs J.E.J., Hill N.H. and Horrocks A.R., 'A study of the global kinetics of thermal degradation of a fibre-intumescent mixture' paper presented at the 8th European Conference on 'Fire retardant polymers', 24–27 June 2001, Alessandria, Italy; *Subsequently Published in Polym. Deg. Stab*., 2002, **77**, 187–194.
50. Ventriglio D.R., 'Fire safe materials for navy ships', *Naval Engn. J*., October 1982, 65–74.
51. Tewarson A. and Macaione D.P., 'Polymers and composites – an examination of fire spread and generation of heat and fire products', *J. Fire Sci*., 1993, **11**, 421–441.

52. Sorathia U., Rollhauser C.M. and Hughes W.A., 'Improved fire safety of composites for naval applications', *Fire Mater.*, 1992, **16**, 119–125.
53. Sorathia U., Gracik T., Ness J., Durkin A., Williams F., Hunstad M. and Berry F., 'Evaluation of intumescent coatings for shipboard fire protection' in Lewin M. (Eds), *Recent Advances in Flame Retardancy of Polymeric Materials*, Vol XIII, Proc. of the 2002 Conf, BCC, Stamford, Conn., 2002.

10
Cost analysis

M D WAKEMAN and J-A E MÅNSON,
École Polytechnique Fédérale de Lausanne (EPFL), Switzerland

10.1 Introduction

Textile composites offer a diverse range of properties suited to an equally wide range of applications, offering the design engineer opportunities for many end-uses. Applications vary significantly in size, complexity, loading, operating temperature, surface quality, suitable production volumes and added value. The expanding choice of raw materials, in terms of reinforcement type (concentration and fibre architecture) together with matrix material (subsets of both thermoplastic and thermoset polymers), followed by many subsequent final conversion processes, gives impressive flexibility. These variables often interact to create for the uninitiated an often confusing material and process 'system'. The properties of the final moulded item are hence controlled by the initial choice of fibre and matrix type, together with the subsequent processing route.

The particular route selected through the choice of fibre type, resin system, processing technique, finishing operations and assembly sequence will not only affect the part performance, but importantly the part cost. For example, a manual-based lay-up process will be suited to low-volume components, whereas for higher manufacturing volumes considerable investment in processing equipment and automation can be made. Material scrap must be minimised. During the design of a component, the processing technique must be selected not only to give the desired geometrical complexity, but also to suit the cost structure of the component under consideration. Notably, the processing technique should be chosen to suit the manufacturing volume over which tooling costs and plant are to be amortised. Hence, for the full implications of any use of textile composites to be considered, both the benefits and costs must be quantified. This is shown schematically in Fig. 10.1.

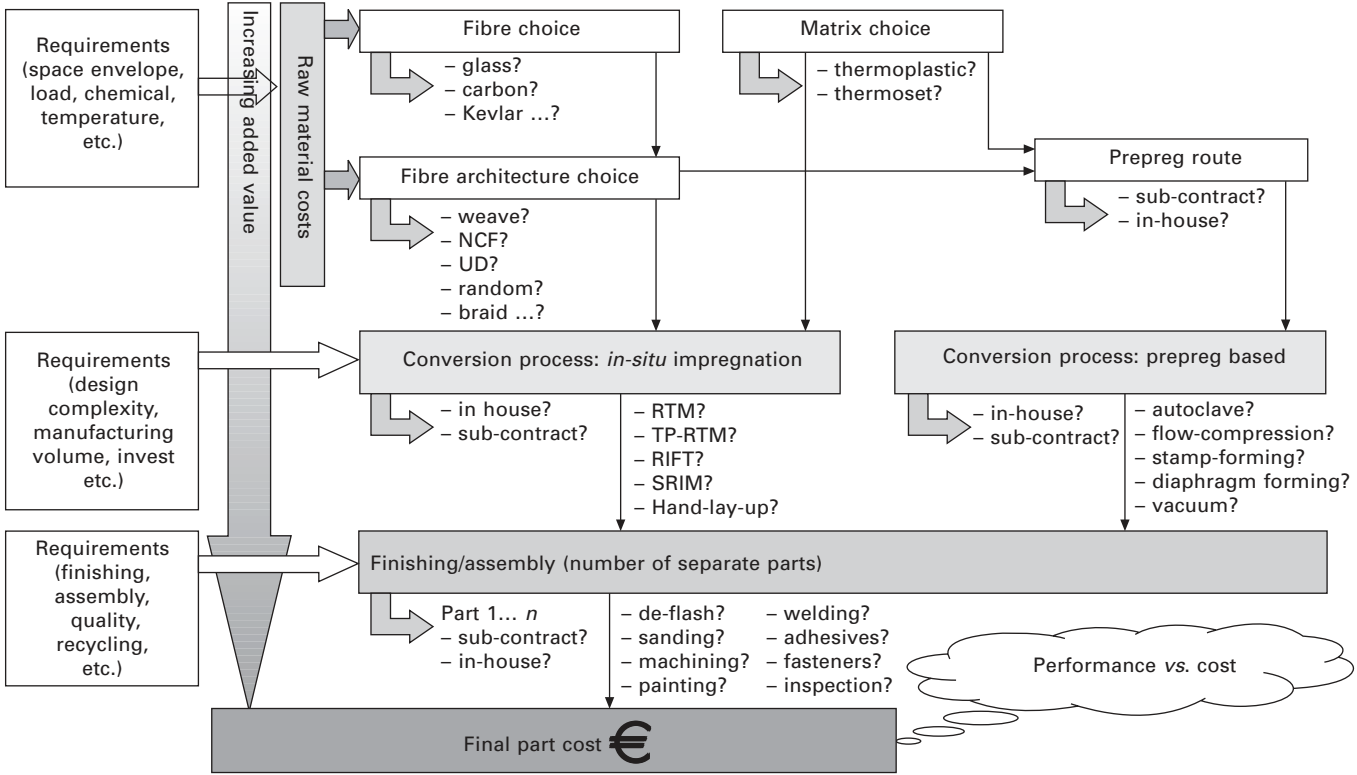

10.1 The decision making route through interacting material, process, property, cost relations.

10.1.1 Outline of this chapter

In order to illustrate different factors affecting the cost of textile composites, a cost modelling tool is described such that the process of cost estimation can be understood. Cost build-up in textile composite applications is then discussed, commencing with an examination of raw material prices. Typical process machine and tooling costs are discussed, followed by a summary of the effect of manufacturing volume on cost and the typical manufacturing volume of textile composite conversion processes. Assembly costs form important cost portions of a module and the effect of parts count reduction on cost is shown. Two case studies are then presented that show the build-up of system cost for components made of textile composite structures:

1. Chassis brace components produced by thermoplastic sheet stamping and over-injection moulding.
2. Carbon epoxy aft fuselage panels for the Airbus A380.

10.2 Cost estimation methodologies

10.2.1 Cost estimation approaches

Cost modelling approaches for composite manufacturing have been reviewed previously[1–3]. Beyond 'rule of thumb' approaches that use experience-based estimating, these can be summarised as comparative techniques[4–8], process-oriented cost models[9–11], parametric cost models[12–15], relational databases[16], object-oriented system modelling tools[17] and process flow simulations[18–23]. An understanding of how these techniques work and of their general suitability is of importance for the realistic modelling of a particular process.

As the basis for examples presented throughout this chapter, a cost prediction tool is described, which will drive an understanding of how cost is built-up in textile composite applications[3]. This parametric technical cost model (TCM) is based in MS Excel™, interacting with MS Visual Basic™. The TCM can be coupled with a discrete event-based process-flow simulation (PFS) tool that dynamically represents the interactions between the different manufacturing operations. Hence, an averaging effect is gained over a statistically significant period, thereby generating input data for the TCM and increasing the accuracy of the cost calculation.

10.2.2 Technical cost modelling

Parametric models offer flexibility together with easy manipulation of process and economic factors for sensitivity studies. Activity-based costing (ABC) accountancy attributes direct and overhead costs to products and services based on the underlying activities that generate the costs. However, as ABC

is based upon historical data, it is of limited use when new processes are considered. In cases where detailed information is not available to define overhead costs, not all variable costs will be activity-based and volume-based approximations are applied (for example, a ratio of direct to indirect labour). Hence, TCM methodologies are related to ABC but use engineering, technical and economics characteristics associated with each manufacturing activity to evaluate its cost[24]. The technical cost modelling approach is shown in Fig. 10.2.

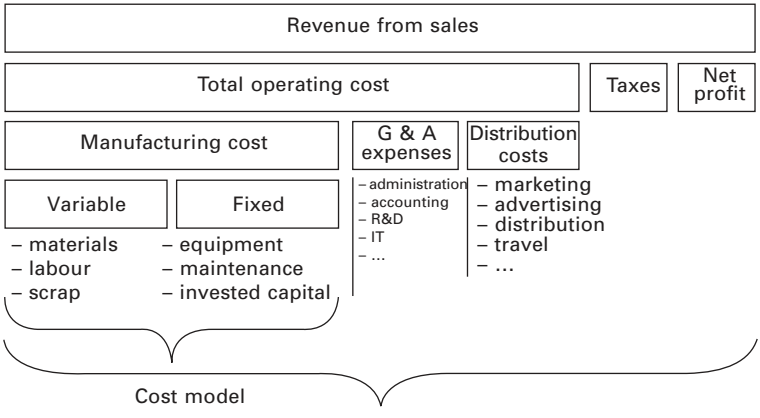

10.2 Technical cost modelling approach.

TCM commences with the identification of the relevant process steps required to manufacture a particular component. The approach is designed to follow the logical progression of a process flow. In this manner, the process being modelled is divided into the contributing process steps. Each of these operations contributes to the total manufacturing cost as resources are consumed. As such, each operation is modelled and the respective total manufacturing cost is divided into contributing cost elements. Hence, the complex problem of cost analysis is reduced to a series of simpler estimating problems. The contribution of these elements to the part manufacturing cost is derived from inputs including process parameters and production factors, e.g. production rate, labour and capital requirements, and production volume. These elements are calculated based on engineering principles, economic relationships and manufacturing variables.

Fixed and variable costs

A natural segregation of cost elements is between those that are independent and those that are dependent on the manufacturing volume within a given time frame. Variable costs are independent of the number of parts produced

on a per piece basis. For example, the raw material cost is generally independent of the number of parts made. Additionally, labour, energy and sub-contracted costs remain constant regardless of production volume.

Conversely, fixed costs are capital investments that are necessary for the manufacturing facility. They are labelled as fixed because they are typically a one-time capital expenditure. These costs are distributed over the number of parts produced and the fixed costs per piece vary according to the production volume. As the production volume increases, fixed costs are reduced because the investment can be amortised over more parts. Machine, tooling, maintenance, cost of capital and building costs are typically fixed costs.

Input data and assumptions

The cost model input data are derived from the PFS output together with additional data concerning materials (e.g. weight fraction, costs), equipment (cost, area, energy, lifetime, maintenance, cost of capital), labour (number of workers, number of shifts, working area) and overheads (consumables, storage, scrap and reject). Input data is entered through a MS Visual Basic™ user interface or directly into the spreadsheet.

The model will predict either the manufacturing costs occurring during continuous production, or the total cost including general and administrative (G&A) overheads (Fig. 10.2). This depends on factors such as the indirect to direct labour staff ratio. Development costs, production tests and machinery installation can be included with 5–10% of the initial machine purchase price per year (covering installation and planned maintenance schedules), or excluded. Machinery is normally assumed new and depreciated linearly, with a typical life of seven and ten years for three and two shift patterns respectively. Production periods of yearly increments are considered. Where applicable, a resale value can be applied to the equipment if production ceases before the defined life. Tool life is defined by a number of parts and hence costs are amortised over the life of the part. Labour costs comprise both direct labour and social costs. An augmented reject rate is used and material costs consist of the product, waste, rejected products and any internal recycling cost or benefit.

Model structure

Figure 10.3 illustrates the structure of the model where multiple materials and machines can be modelled. For example, several manufacturing cells can be modelled, with separate finishing and assembly steps. This would correspond to a manufacturing plant divided into cells, such as shown in Fig. 10.4. The manufacturing plant is described further in section 10.4 to illustrate the method of breaking down the overall estimation into the individual steps.

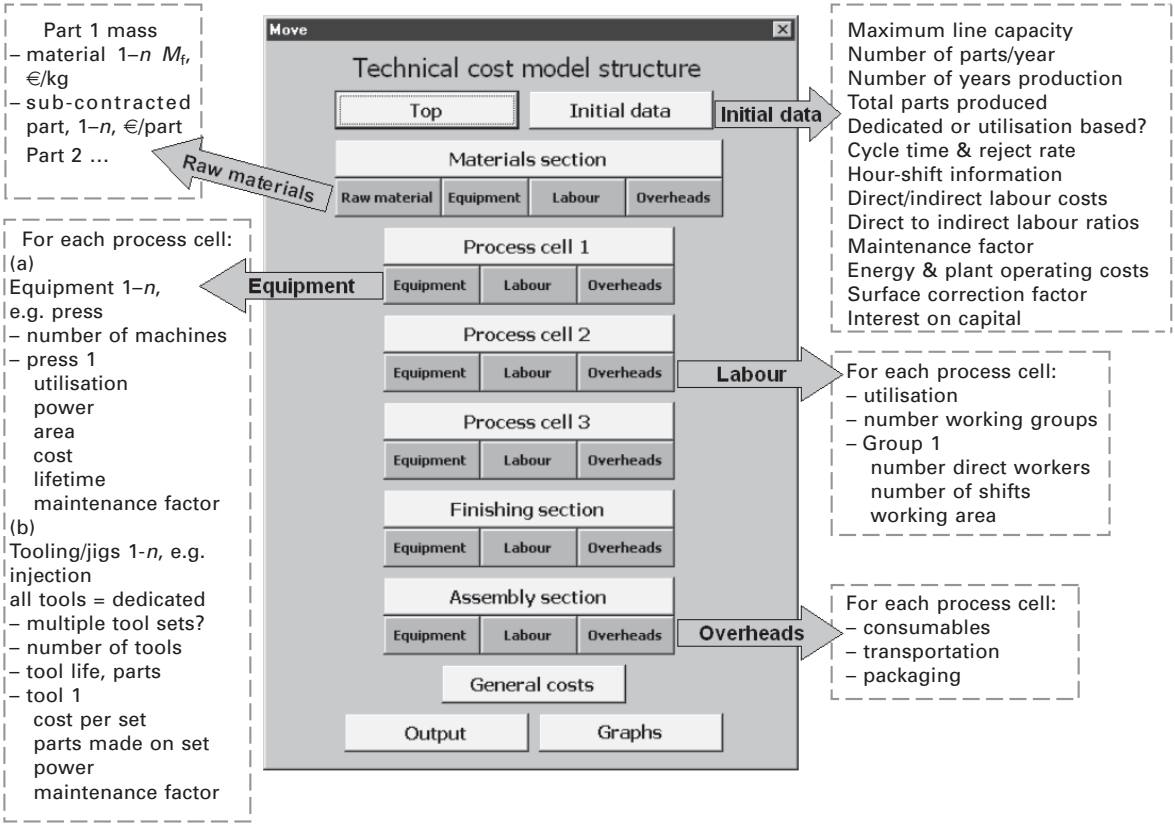

10.3 TCM structure and principal input fields. M_f = fibre mass fraction.

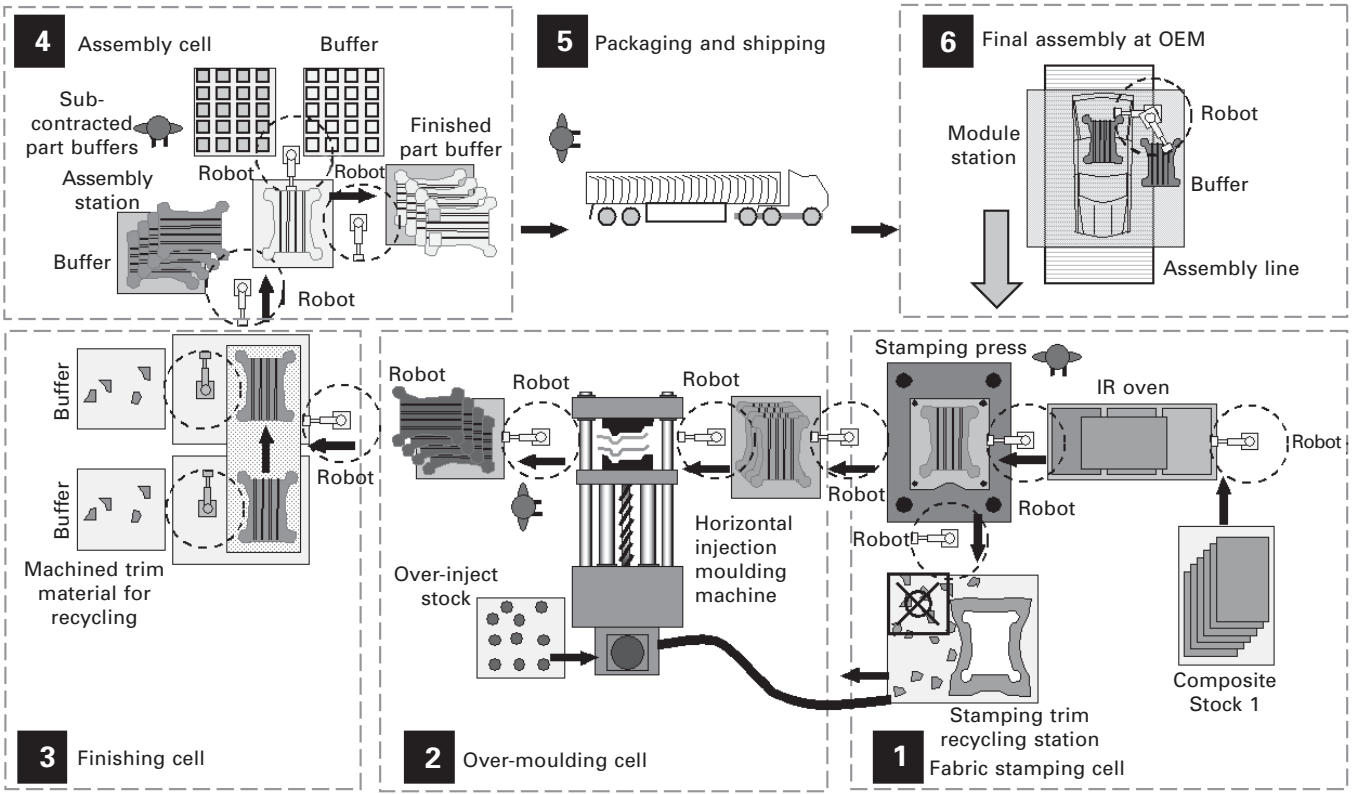

10.4 Schematic of a composite manufacturing line: combination of thermoplastic stamping with over-moulding, trimming, module assembly, shipping and body-in-white (BIW) assembly operations.

The TCM developed enables the amortisation of plant costs to be approached in two ways. First, a whole line could be dedicated to one product where all of the fixed plant costs are amortised over the number of parts produced for the total years of production. Cost against volume graphs can be generated simply by assuming that the full plant costs are spread over the parts produced, with strongly increasing costs at lower volumes. In the second case, only a fraction of either a line capacity or a plant would be assigned to one product while the remaining capacity would be sold to a second client. Fixed plant costs are amortised as a fraction of utilisation and the number of years that the plant is used, effectively giving a charge rate per minute for a manufacturing line.

Cost model output

The TCM enables factors, including equipment cost, depreciation and operating power, to be defined and sensitivity analyses to be performed for the whole line or sub-units of a manufacturing cell. The model predicts the manufacturing cost and cost segmentation as a function of volume. Cost versus volume relations are given together with segmentation of the total production cost into:

- material;
- direct labour;
- overheads (indirect labour and plant costs);
- depreciation, interest and maintenance;
- energy;
- consumables;
- tooling;
- transportation;
- sub-contracted costs.

Additionally, for each process step, costs can be further segmented into the above categories, and the material costs itemised. Other outputs of the cost model are global scrap and reject rates, production cycle time, production time, production rate, plant area and energy requirements.

10.2.3 Process-flow simulation tool

While cost calculations do not require input from process-flow simulations, a limitation of the parametric technical cost modelling approach is the assumption that each step in the manufacturing process operates independently from the others from a temporal standpoint of part flow in the manufacturing line. This assumption often results in an underestimation of the manufacturing cost[23]. This is overcome by PFS, which dynamically represents the interactions

between the different manufacturing operations, gaining an averaging effect over a statistically significant period (depending on the number of parts made), rather than a simple 'static' representation. PFS includes commercial codes such as Witness™. Benefits include the ability to predict the cycle time and the capacity of the process, in addition to the manufacturing cost. These tools can also aid process improvement studies, identify bottlenecks and achieve a better distribution of personnel and raw materials on the shop floor.

Again, as a basis for the examples presented in this chapter, the PFS tool developed is briefly described. It is a discrete-event simulation tool written in MS Visual Basic™, consisting of a hierarchical structure in the way that a commanding finite state machine controls other finite state machines, which represent the objects in the line. Such simulations are used to simulate components that normally operate at a high level of abstraction[25]. Discrete-event simulation is relatively fast while still providing a reasonably accurate approximation of a system's behaviour.

PFS input and operation

The tool consists of a workspace where the user places all the objects (machines, buffers, robots, workers, etc.) that have an influence on the production flow of a given manufacturing line (e.g Fig. 10.4). The modules are, for example, machines, robots or buffers. Machines are preceded and followed by a transfer system, such as a robot. Graphic objects are descriptive symbols that are not part of the process flow. The end category is the final part buffer and the end of the simulation. Failure incidents can be simulated, where the user defines a failure probability and the time needed to fix the problem. The program randomly generates breakdowns according to these data. Both operators and workers can be considered. Workers are fully engaged in the manufacturing line and are part of the actual manufacturing process. Operators perform maintenance and problem-solving tasks. Their occupancy level is predicted by the failure generation function, enabling optimisation of operator allocation. Both convergent and divergent material or part flows are possible using different combinations of objects, with the following categories included:

- graphic object;
- processing machine;
- buffer;
- materials stock;
- end;
- continuous conveyor;
- indexed conveyor;
- single transfer;

- multiple transfer;
- unloading task;
- loading task;
- jig.

All these objects need to be defined. Figure 10.5 gives examples of PFS input data for a buffer, process machine and a transfer device for a section of the line in Fig. 10.4.

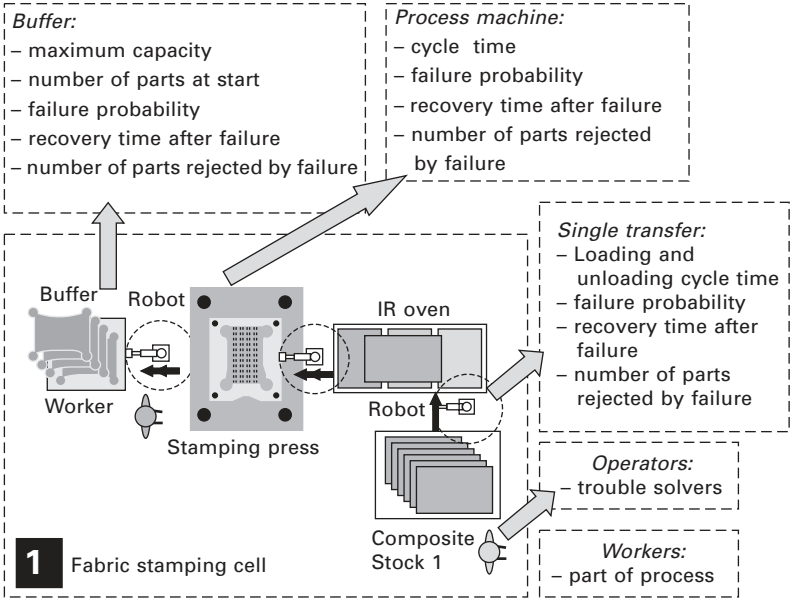

10.5 PFS input data for buffers, transfer devices and processing machines.

Either a time goal or an output goal (a number of parts) can be selected which defines the end point of the simulation run. Input data are stored in a MS Access™ database before the program processes the data. The program moves forward in time steps (simulated seconds) through each object in a user-defined sequence. Events (incidents that cause the system to change its state in some way) can occur only during a distinct unit of time during the simulation and not between time units. According to the category or type of an object, a function is run that virtually checks the objects and adjusts their simulation variables. When the simulation goal is reached, values of the simulation variables are written into a MS Excel™ template.

PFS output

The results are processed by MS Excel™ macros giving information about: the global production scenario (e.g. production cycle time), the detailed object (e.g. number of parts processed or loaded, machine utilisation, buffer start/finish size), the number of produced parts, the time needed for production and the average cycle time of the line. Furthermore, process and throughput time are calculated considering any scheduled maintenance. Occupancy represents the relative time an operator is performing maintenance due to unscheduled stoppage. These results can then be transferred to the TCM. Hence, as a first step in a cost calculation, a PFS can be performed to generate input data for a subsequent TCM, thereby increasing the accuracy of the cost calculation.

10.3 Cost build-up in textile composite applications

10.3.1 A materials perspective

Following the sequence of the TCM (Fig. 10.3), the quantity and cost of the textile composite raw materials are required. Thus, defining the raw material cost is one of the steps needed towards calculating the system cost. The data in Tables 10.1 and 10.2 are intended for use as input into a full TCM and *not*

Table 10.1 Typical composite raw material costs: un-impregnated textiles and polymers

Reinforcement	€/kg	Matrix	€/kg
Glass	1.6	Polypropylene (PP)	0.7
Carbon (80k–12k)	15–17.5	Polyethylene terephthalate (PET)	3.5
Kevlar	23	Polyamide 66	2.5–4
		Polyamide 12 (PA12)	8.4
GF weave (1200 tex, 300 g/m^2)	10	Polyetherimide (PEI)	17.6–22
Kevlar weave (300 g/m^2)	47	Polyetheretherketone (PEEK)	68–77
CF weave (HS 12k CF, 300 g/m^2)	78	Unsaturated polyester	1.5–1.8
CF weave (IM 12k CF, 300 g/m^2)	124	Vinylester	2.5–3.5
GF NCF (100″ wide, 1000 g/m^2)	3	Epoxy	2.2–55
Commercial 12k CF NCF (100″ wide, 1000 g/m^2)	17–30	Phenolics	1.65–5
Aerospace 12k CF NCF (100″ wide, 1000 g/m^2)	45	Cyanate esters	62
GF biaxial braid	11–15	Polyurethanes	5.5–14
CF biaxial braid	31–90	Bismaleimides (BMI)	78

GF, glass fibre; CF, carbon fibre; NCF, non-crimped fabric.

Table 10.2 Typical textile composite raw material costs: semi-finished products

Thermoplastic-based textile composites			Thermoset-based textile composites		
Material form	€/kg	Example of supplier	Material form	€/kg	Example of supplier
CF/PA12 sheet	50–54	Schappe Techniques	GF/epoxy, woven prepreg, 720 g/m^2, 1 m × 50 m roll	26	SP systems, also: Hexcel Cytec
GF/PA12 sheet	13–17	Bond Laminates TEPEX	CF/epoxy unidirectional (UD) prepreg, 476 g/m^2 (CG carbon), 1 m × 150 m roll	29	SP systems, also: Hexcel Cytec
CF/PA66 sheet	30–50	Bond Laminates TEPEX			
GF/PA6 sheet	7–11	Bond Laminates TEPEX	CF/epoxy, UD prepreg, 461 g/m^2 (HM carbon), 1 m × 150 m roll	91	SP systems, also: Hexcel Cytec
GF/PET sheet	4.6–7.5	Vetrotex	CF/epoxy, UD prepreg, 461 g/m^2 (HM carbon), 1 m × 150 m roll	91	SP systems, also: Hexcel Cytec
GF/PP dry fabric	3–4.5	Vetrotex			
GF/PP sheet	3.5–5.5	Vetrotex			
GF/PP sheet, GMTex	3.5–5.5	Quadrant Plastic Composites	Aramid/epoxy UD prepreg, 545 g/m^2, 1 m × 150 m roll	50	SP systems, also: Hexcel Cytec
GF/PP UD tape	4.9–6.4	Plytron	CF/epoxy, woven prepreg, HS carbon), 517 g/m^2, 1 m × 50 m roll	59	SP systems, also: Hexcel Cytec
PEI/GF & PPS/GF	60	CETEX sheet (Ten Cate)	CF/epoxy, woven prepreg, HS carbon), 517 g/m^2, 1 m × 50 m roll	59	SP systems, also: Hexcel Cytec
PEI/CF & PPS/CF	140	CETEX sheet (Ten Cate)	Closed cell styrene acrylonitrile (SAN) core material, 5 mm, 50 kg/m^3	10/m^2	ATC
CF/PP tape	16–29	GuritSuprem/ Flex composites	Closed cell styrene acrylonitrile (SAN) core material, 30 mm, 50 kg/m^3	41/m^2	ATC
CF/PA tape	20–30	GuritSuprem/ Flex composites			
CF/PET tape	20	GuritSuprem Flex composites			

as a cost-based materials selection guide. Costs will vary with: oil price, polymer/fibre price, exchange rates, the application dimensions (*vs*. sheet or roll dimensions), and weight of material sold (20 boat hulls *vs.* an order for 200 000 automotive components/year for seven years). Suppliers are given as examples only and costs should be taken as commonly accepted representative guidelines rather than formal prices of any supplier.

10.3.2 General input data

The second step in the sequence of the TCM (Fig. 10.3) is to define the general input data for the manufacturing plant. Such data obviously vary with industrial sector, the manufacturing processes used and the planned production volume. This typically includes the following factors, which are determined on a case basis:

- maximum line capacity/yr;
- number of parts/yr desired;
- number of years production;
- reject rate;
- part cycle time;
- working days/year;
- number of shifts and hours/shift;
- combined direct and indirect labour costs including social;
- ratio indirect/direct labour staff;
- energy costs;
- plant operating cost per unit area;
- equipment maintenance;
- interest on capital.

10.3.3 Effect of manufacturing volume

The industry sector considered has an important role in composite manufacturing process selection. If it is assumed that the manufacturing line does not normally exist (compared with the highly established steel and aluminium manufacturing industries), then costs must be calculated on a dedicated basis. The effect of this is discussed further in section 10.4.5.

The fixed costs associated with setting up a manufacturing line need to be considered against the number of parts that need to be produced. Components produced at higher annual volumes will justify the use of automated equipment and robotic transfer systems, for example, the stamping of thermoplastic composites for automotive applications. In contrast, components produced at lower annual volumes, such as for niche marine products, often use increased manual labour (typically €30/h in Europe) rather than automation as high fixed costs would be amortised over uneconomic volumes.

Figure 10.6 shows an approximation of the parts produced per year from one tool set for different thermoplastic and thermoset-based textile composite processes. As the maximum manufacturing volume increases, the fixed costs also tend to increase. While high fixed cost processes can be used at lower volumes, it may not be the most economic approach. An exception to this would be the thermoset-based automated tape placement (ATL) and automated fibre placement (AFP) processes, where the fixed costs are high and the volumes low, justified by reduced material scrap of expensive aerospace grade carbon prepreg tape.

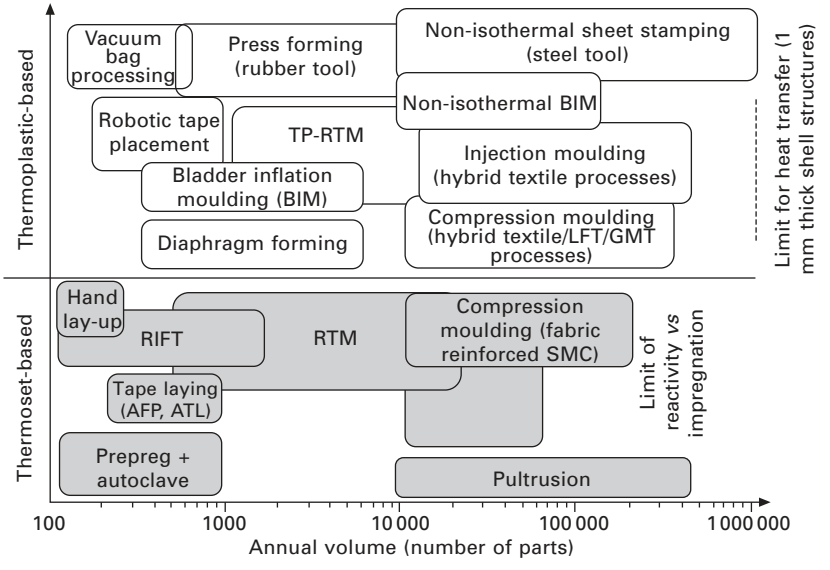

10.6 Textile composite annual manufacturing volumes (adapted from Månson *et al.*[26]).

Assuming 235 to 250 working days per year, and 90% efficiency, the effect of process cycle time on the number of parts produced per year from one tool set can be modelled for: one shift (7.5 h/day), two shifts (15 h/day) and three shifts (22.5 h/day). Figure 10.7 shows that processes requiring long cure times in ovens or autoclaves will be limited to low volume, high added value, applications. In contrast, thermoplastic composites can offer material and process combinations with cycle times of 1 (stamping glass fibre reinforced polypropylene (GF/PP) systems) to 5 min (rubber forming of carbon fibre reinforced polyetherimide (CF/PEI) sheet), giving low machine and tool costs per part.

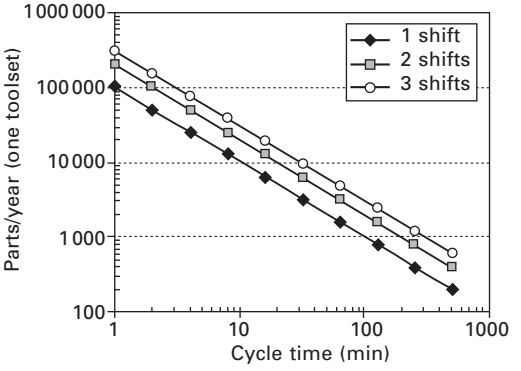

10.7 Effect of process cycle time versus maximum parts produced per year, for one-, two- and three-shift patterns.

10.3.4 Typical process machine cost

Any cost calculation requires identification of the process equipment needed, including machines, transfer devices and buffers, such as those shown in Fig. 10.4. Relations can be established between, for example, press size in tonnes and press cost to give general guidelines for equipment costs. Table 10.3 includes examples of textile composite equipment costs, which are size and application dependent. Specific information is used for each case.

Table 10.3 Typical textile composite process machine costs

Equipment	Cost
Braiding machine (172 carriers)	€250–350k
100″ (2.5 m) warp knitting machine	€1500k
1500 tonne hydraulic press	€900k
IR oven	€150k
Vacuum pump and tank (1–2 m^2 part, 30/day for 1 yr)	€6.1k*
RTM injection unit (high volumes)	€170k (€40k for lower volumes)
Autoclave, small	€230k
Automated fibre placement (AFP)	€5000k

* Not consumables.

In order to show typical utilisation-based equipment costs (part and size specific), a range of machine costs per minute has been calculated. This assumed a three-shift pattern with full utilisation and a seven year production period, with inclusion of plant surface costs (€85–115 m^2/y), energy costs (€0.05–0.12/kW h), and cost of capital for the machines. Direct operators and indirect overheads were excluded. The results are given in Fig. 10.8.

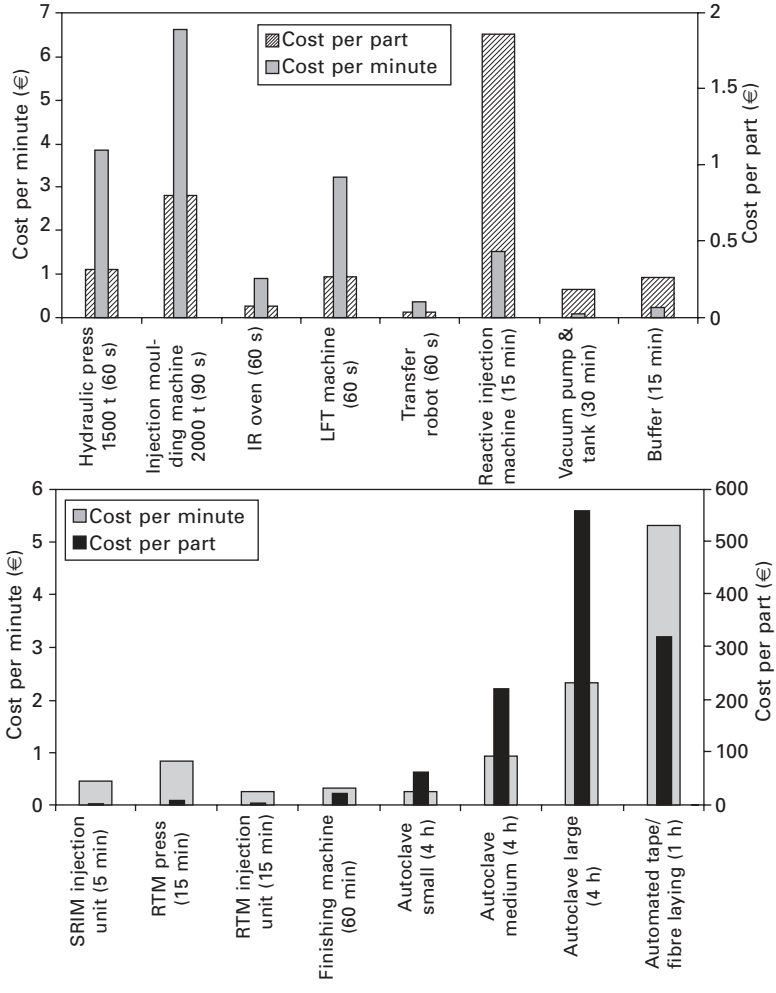

10.8 Examples of textile composite utilisation-based equipment cost (part and size specific), machine cost/min based upon: three-shift pattern, full utilisation, seven year production period, including: plant area cost, energy cost, cost of capital for the machine, *excluding* direct operators and indirect overheads.

10.3.5 Tooling costs

Tooling costs are an important issue for composite processing. Many textile composite techniques, notably for thermoset-based materials, have cycle times of several minutes (structural reaction injection moulding, SRIM) to several hours (autoclaving of prepreg) and tooling cost is a significant fraction of the total. The use of low-cost tools (e.g. nickel shell composite tools) can reduce costs compared with steel tools, especially for lower manufacturing

volumes. For example, tooling costs of €920k for a resin transfer moulding (RTM) floor pan amortised over 13 000 parts/yr (the maximum from one tool set on a two shift pattern with a 15 min cycle time) for five years production (total parts = 65 000) would give a tooling cost of €25/part (including tool maintenance). A lower-cost, epoxy-based tool at €250k would reduce the tooling cost to €6.9/part. However, if the cycle time for the steel tool were reduced to 10 min, such that 20 000 parts were made per year, then the tooling cost per part would be €17/part. A general increase in cost competitiveness occurs when the manufacturing volume from one tool set is increased. For example, thermoplastic textiles can be stamp-formed with over 200 000 parts/yr from one tool set (€500k), giving a tooling cost of €0.9 (seven years' production). In comparison with steel stamping processes that have multiple tool sets, such composite processes offer lower tooling costs. High volumes with thermoset-based processes will need multiple tool sets and handling equipment. While multiple moulding cells using multiple tool sets are used in production, generally a process should be used that is adaptable to the manufacturing volume to avoid large moulding plants with many tool sets.

10.3.6 Effect of process scrap

An important cost issue with textile composites is that of material scrap. This is not the reject rate of the final conversion process, for example RTM, but that of preparing the preform. Taking the example of a RTM floor plan (16 kg), carbon fibre preforms could be taken from non-crimp fabrics (NCFs) to produce the structure. Even when using computer-optimised nesting patterns, NCF waste fractions of 30% can occur. With NCF costs forming 63% of the total floor pan cost, at an NCF cost of €30/kg, this can represent €80/part of waste. Reduction of fabric scrap, ideally before moulding, or maximising the value of the material post-process, are key to the economic use of non net-shape textile preform composite processes.

10.3.7 Assembly costs

Composite materials enable many features to be integrated into a single composite component. A 10:1 component consolidation is achievable but the added complexity in operations such as blank placement (for stamp forming) and preform construction (for RTM) should be assessed to evaluate the effect on cost (reduced parts count with a complex part *vs*. increased parts count with simple parts)[27]. Parts consolidation minimises tooling and parts count and the associated investment, inventory, tracking, and assembly effort and space. The reduced count of tools, jigs and fixtures can both increase the flexibility of assembly operations, simplifying the process of assembling

model variants on the same line, and reduce the number of assembly steps.

Simply modelling a composite component cost and comparing this with an existing (metallic) product often results in an underestimation of the potential cost saving for a composite system compared with a steel system. The TCM approach consists of two sections (Fig. 10.9), where part 1 focuses on component costs and part 2 on the assembly cost to give a system cost. This requires definition of assembly scenarios, often based on a modular approach, to fully develop the system cost and the final weight-saving implications.

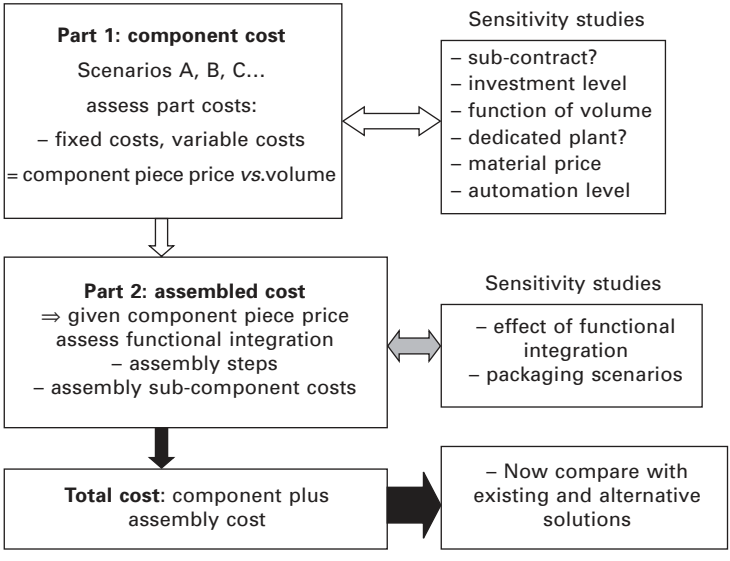

10.9 Cost modelling approach: Part 1 = component cost, Part 2 = module cost.

In a high-volume assembly line a reduction in the line length or the number of assembly workers allocated to a particular task can reduce the system cost. Comparison of a conventional steel system with a modular composite system can show considerable cost savings at the assembly stage (Fig. 10.10). As an example, a robot could be used to mount a one-piece composite moulding in a simple operation rather than the four stations and workers required to fit a metallic-based part. For a two-shift pattern assembling 500 modules per day, a comparison between the alternatives illustrates the point of considering the system cost. With typical line investment costs of €5000/m^2 and associated surface costs, with four workers included (and associated indirect costs), the costs of manual assembly would be considerable at €7.1/part. By assembling a drop-in module via robot on such an assembly line, assembly costs could be reduced to €1.1/ part.

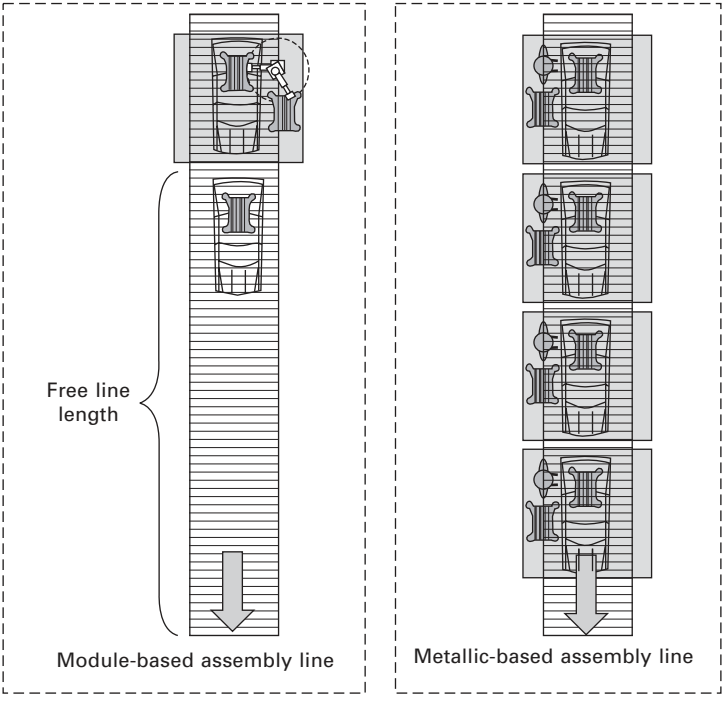

10.10 Assessment of assembly costs: cost reduction by functional integration, parts count reduction, and modular assembly.

10.4 Case study 1: thermoplastic composite stamping

10.4.1 Ford Thunderbird X-brace component

Using the TCM approach described in section 10.2, comparative cost estimations were made for X-brace components used to stiffen cabriolet body-in-white (BIW) assemblies, produced from different *candidate* composite materials. The prime application was the Ford Thunderbird, with a target manufacturing volume of 20 000 units per year. The existing steel X-brace formed baseline cost, assembly cost and mass values (Table 10.4).

Table 10.4 Steel X-brace system details

Item	Weight (kg)
Steel X-brace	15.6
Steel panel	3.6
Assembled to BIW: system mass and cost/part	19.3

Figure 10.11 shows the Ford Thunderbird vehicle and the steel X-brace assembly, where a steel tube-based brace mounts onto suspension towers. A vertical steel panel spanning the width of the vehicle attaches to the shock towers. The candidate system examined in this cost study is a composite replacement (Fig. 10.11) that could combine the X-brace and the vertical panel, but would use the existing steel suspension towers. A fibre-reinforced thermoplastic sheet would first be stamped to give a component of complex double curvature. To maximise the stiffness of the component, a ribbed structure would be over-moulded onto the stamped sheet, using the same polymer as the fibre-reinforced sheet matrix[28].

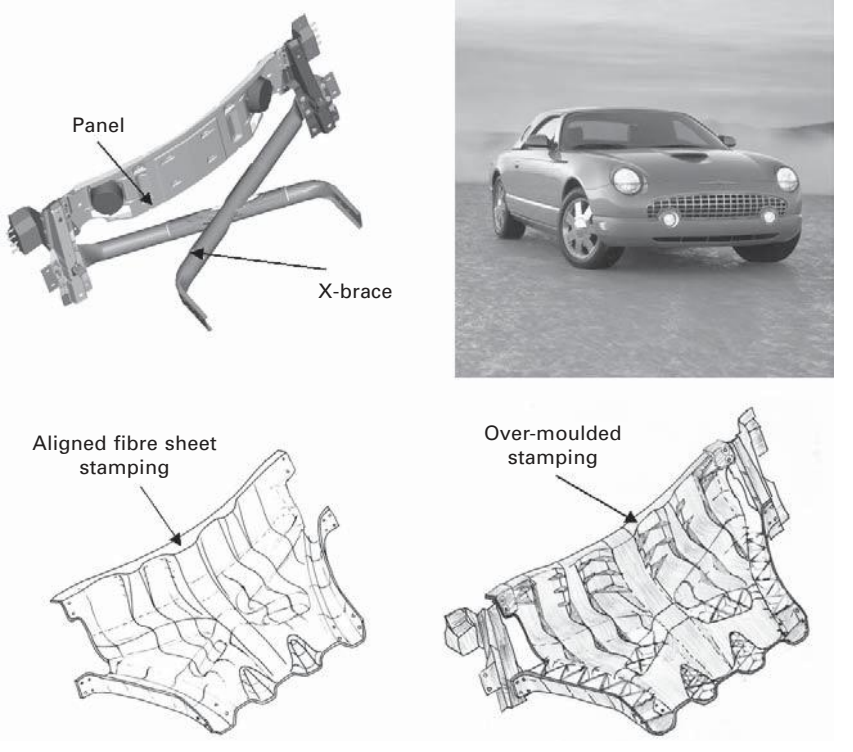

10.11 Ford Thunderbird X-brace in steel and a *candidate* thermoplastic composite solution.

10.4.2 Thermoplastic composite material systems

Three material systems were examined, all consisting of thermoplastic composite prepreg sheets processed via non-isothermal stamping, followed by an over-injection moulding process incorporating closed loop recycling of stamping scrap. GF/PP sheet, commercially available as Twintex™, formed

a benchmark system. In order to decrease the component weight and offer higher operating temperatures potentially compatible with steel E-coat and paint line temperatures, a glass fibre reinforced polyethylene terephthalate (GF/PET) sheet material (PET Twintex™) was studied. The third material, offering the greatest weight-saving potential, was a carbon fibre reinforced polyamide 12 sheet product (CF/PA12). The over-moulding phase, for all three material variants, used recycled stamping waste diluted with virgin polymer, giving fibre mass fractions of 30–40%. Typical sheet material costs are shown in Table 10.2 and over-moulding polymer costs in Table 10.1. As a reference, automotive grade sheet steel is €0.9/kg.

Sheet cost estimates for a reactive impregnation route

Costs of existing CF/PA12 fabric grades were greater than could be justified for this particular application, but the properties that CF/PA12 could offer were still considered of interest and hence an alternative material supply route was invested using TCM techniques. This study was based around the ability to batch pre-impregnate sheets at a laboratory scale via a reactive thermoplastic RTM process using an anionically polymerised laurolactam system (APLC12)[29–31]. Commercialisation would require a continuous reactive impregnation unit to produce sheet material. Line speeds for a novel prepreg line were predicted, based upon experimental results, and modelling of the reaction kinetics coupled with impregnation phenomena (including capillary forces). With a given line speed (>3 m/min), these results were coupled with the TCM to calculate the sheet cost, based upon an estimated line cost of €2000k, the surface area and labour needed, and the energy costs. Automotive grade carbon fibre (€15/kg), weaving costs and APLC12 material costs were used as raw material inputs, with the line running costs and an additional profit factor that would be added by any commercial producer of such sheet material. Depending of the machine utilisation, a material cost of €22/kg was predicted, which offered cost reductions compared with existing CF/PA12 systems.

10.4.3 Weight saving assumptions

Prior to a full design study and finite element analysis (FEA) modelling, weight-saving assumptions (Table 10.5) were made compared with the existing steel X-brace system, to determine the initial cost case for a composite X-brace. From these assumptions, the average part thickness was calculated, assuming a final ratio of stamped material to over-moulded material of 60:40. Note that local increases in section thickness occur, for example to facilitate load introduction. The part thickness is an important variable in the later manufacturing cost prediction, where an excessive thickness will

Table 10.5 Weight savings from thermoplastic composite material systems

Composite solution	CF/PA12	GF/PET	GF/PP
Stamped sheet thickness (mm)	1.7	2.0	2.8
Average over-moulded polymer thickness (mm)	1.2	1.6	2.4
Composite part weight (kg)	7.7	12.5	13.5
Weight saved (%)	60	35	30
Raw material cost (€)	153	58	44

require longer in-mould cycle times to accommodate shrinkage and reduce warpage.

The stamping process uses a blank-holder system, and as a base line, 30% of the initial stamped sheet was assumed to be scrap material. With closed-loop grinding of this stamping scrap for over-injection moulding, the additional virgin polymer fraction mass has been calculated to give the required thickness. The raw material costs (i.e. before the manufacturing processes of stamp-forming and over-moulding) for the X-brace component in different material systems are hence given in Table 10.5.

10.4.4 Manufacturing process

Figure 10.4 shows an envisaged manufacturing plant for producing the X-brace component. This cost comparison examines steps 1–3 and 5. Production was planned for a five-year period, using a three-shift pattern. A stamping cycle time of 50 s was assumed (3 mm average sheet thickness, 40 s in mould, 2×5 s transfer). The over-injection moulding cycle time was assumed as 90 s (allowance for locally thicker sections, 80 s in mould, 2×5 s transfer), giving a line cycle time of 90 s per part. The maximum number of parts/yr from one set of tools per machine is hence 205 000.

Starting from *composite stock 1*, pre-impregnated thermoplastic sheets are taken from a buffer by a *robot* and placed into an *infrared oven*. The materials are heated above their melting point before rapid transfer to a fast-acting *hydraulic press*, again via *robot*. The press closes and the hot thermoplastic prepreg is shaped to the steel tool profile, in cycle times of 10–30 s for thin shell structures. A blank-holder is used to hold the stamping material. The component is punched out of the overall shaped blank, giving scrap material. The scrap is removed via a *robot* and placed into a chopping and *grinding cell* that processes this scrap prepreg into pellets. This high-volume fraction material is combined with virgin injection moulding pellets to give the desired material for the over-injection stage. The stamped preform is hence transferred via *robot* into a *warm buffer*, which is to ensure that the average temperature at the interface of the stamped material and the over-

injected material is above the composite matrix system T_m. Transfer by robot into the *over-injection moulding machine* enables over-moulding of the complex features. The net-shaped component is removed from the tool by *robot* and loaded onto a *conveyor system* that transports the part to the *trim and machine stations*, where any limited finishing of the net shape part is made, as required, and the finished parts are loaded by *robot* into a *buffer*. This can then be followed by assembly of subcontracted modules as required (this is not modelled in this example).

Quotations were received for the process machines including purchase price, maintenance details, plant floor area, operating power and reject rates where appropriate. As a summary, the stamping (including the recycling cell), over-injection and trimming cells represented investments of €1250k, €3365k and €200k, respectively. Plant areas and powers were: (233 m^2, 259 kW), (229 m^2, 530 kW), and (50 m^2, 100 kW) respectively for the three cells. Tooling quotations for the stamping and over-injection moulding tools were €130k and €500k respectively. All tooling costs were dedicated, while the manufacturing line was used on a cost per minute basis where it was assumed that the remaining 90% line capacity for the five-year production period and the full capacity for the remaining period of plant life were filled by a different client and product, but using nominally the same moulding process. As section 10.4.6 shows, dedication of an automated plant with heavy processing equipment with low utilisation levels results in substantially increased costs. Manual workers are shown in the plant diagram. Transportation costs of €3/part and subcontracted steel load introduction washers at €1/part were included.

10.4.5 Effect of material type

Using the material weight and cost given in Table 10.5, X-brace component cost in the three material types was calculated. Conversion costs will typically be higher for engineering polymers, such as PET, compared with PP. In contrast, the increased wall thickness required for GF/PP, particularly compared with CF/PA12, would increase cycle times for the GF/PP material.

Figure 10.12 shows the effect of material type on part cost. For each material type, a high, medium and low cost boundary is shown. The high case considers increased equipment investment and higher raw material costs while the lower case considers lower equipment and raw material costs. As Fig. 10.12 shows, the lowest part cost was for a GF/PP X-brace structure, at €70/part for 20k parts/yr. Materials costs formed 63% of the total (for the median cost case), and tooling 16%, with 11% for equipment. As the structural performance of the raw materials increased (and temperature rating for PET), so did the part cost (in the materials category), with part prices of €83 and €179 for the GF/PET and the CF/PA12 systems respectively.

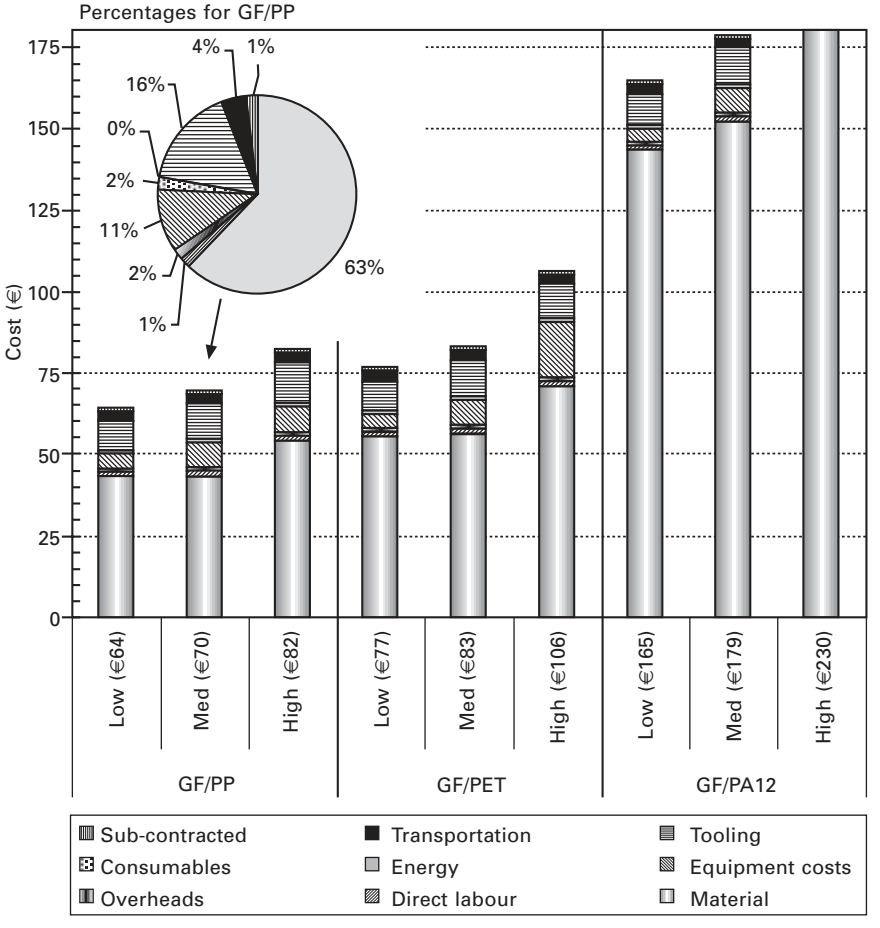

10.12 X-brace part cost segmentation for GF/PP, GF/PET and CF/PA12 material solutions.

An increased weight saving corresponded to an increased cost. The euros needed to save 1 kg of weight (over GF/PP) were €6/kg for PET and €23/kg for CF/PA12 variants. The total investment per part, ranged from an additional (compared with GF/PP) €13/part for GF/PET, to €109/part for CF/PA12. The large total cost increase for CF/PA12 is due to the high absolute mass saved versus GF/PP of 5.8 kg.

10.4.6 Plant utilisation: dedicated *vs.* utilisation based

The overall strategy of a manufacturing plant is an important assumption to set at the outset of any TCM study, with the effect often influencing other manufacturing parameters. The assumption used in this case study is that X-brace production would occupy a percentage of an existing plant capacity,

with the X-brace product hence paying on a cost per minute basis. This enables high-throughput thermoplastic stamping and over-injection moulding processes to be used for a medium volume (20 000 parts/year) application, which would be uneconomic if a manufacturing line capable of over 200 000 parts/yr were used at 10% utilisation. This assumption holds for existing manufacturing processes or where exclusivity for a particular technology is neither held nor desired. However, if a new technology has been developed that requires a new integrated plant to be built to gain maximum cost benefits, then the product must pay for the whole line cost. This also applies if exclusivity is desired, such that the supplier is not permitted to use the same process technology for another client.

Hence the effect of either a *percentage line utilisation* or *amortising the full line costs* is shown to illustrate the importance of this effect.

Where a percentage of the line is attributed, the plant costs (initially assuming all new equipment) are calculated as a function of the use rate. It is assumed that the plant has a life of seven years (three-shift pattern). The remaining production capacity for the years that the X-brace is produced and the full remaining capacity for the final years of the plant life are assumed to be fully utilised by different products by the same or a different client.

Where the full line costs have been considered, X-brace production is assumed to last for five years. Hence the plant life is set to a period of five years. Even for lower production volumes, such as 20k/year, the full plant cost is attributed to the part. Labour costs are also fully attributed to the one product, as the workers are hired to run the plant and cannot be reallocated (assuming a dedicated stand-alone plant). However, energy costs are obviously calculated based upon the running time of the machines needed to produce the total number of parts. At the end of X-brace production, here set as five years, all plant has zero value. An obvious consideration is that a dedicated plant set-up to produce 20k parts/yr would not have the same shift pattern and labour levels as a plant set-up to produce 200k parts/yr. Hence for up to 70k parts/yr, a one-shift pattern has been used, a two-shift pattern used from 70k to 135k parts/yr, and a three-shift pattern used from 135k to 200k parts/yr.

Using common input data for both dedicated and utilisation-based scenarios, but changing the plant life, percentage plant utilisation and shift information, comparisons were made for processing the commingled GF/PP weave, followed by over-injection moulding.

Utilisation-based plant

Figure 10.13 shows cost versus volume curves for five plant assumptions. Costs for a utilisation-based plant are shown, together with a dedicated plant, with the volume portions of the three different shift patterns. The maximum parts/yr that can be made with one-shift is 70k, so for higher

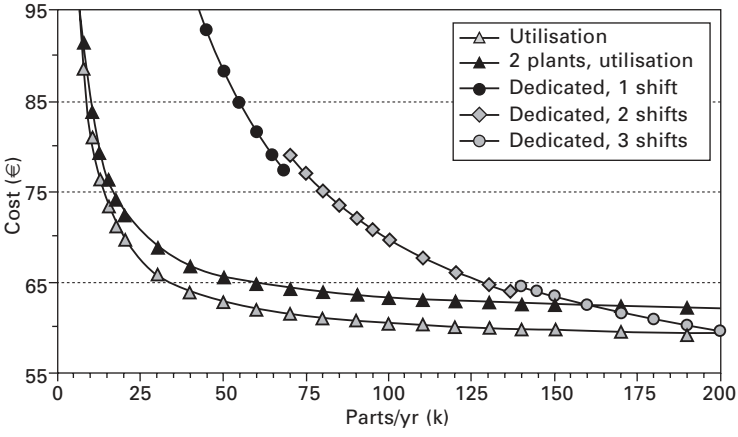

10.13 Effect of plant dedication or utilisation scenario on part cost versus volume.

volumes a two-shift pattern is needed, increasing cost at 70k, but quickly giving cost reductions when more than 80k parts/yr are made up to the two-shift pattern limit of 135k. From here on, a three-shift pattern can be used to the maximum of 200k parts/yr. However, a utilisation-based plant always gives a lower cost.

The utilisation-based cost versus volume curve in Fig. 10.13 for GF/PP shows that part costs for this hybrid moulding process reduce steeply to 20k parts/yr (€70/part). From 20k to 50k per year (€63/part), part costs reduced by 10%. From 50k to the maximum one-tool volume of 200k units per year (€59/part), a further reduction of 7% occurred. With only a 7% cost shift between 50k and 200k parts/yr, the hybrid moulding process is suited to a wide range of manufacturing volumes. If higher volumes than 200k parts/yr were required, additional processing cells (utilisation-based) and tool sets (dedicated) would be needed. Higher costs at lower volumes were principally due to the amortisation of tooling costs over the lower manufacturing volume, with all equipment costs on a percentage utilisation basis.

Dedicated plant scenario

Figure 10.14 compares cost breakdowns for volumes of 20k and 200k parts/yr, for both dedicated and utilisation-based operations. Where 20k parts/yr are produced, the cost per part increases by 151% for a dedicated plant used for five years (one-shift pattern) compared with a utilisation-based plant at 200k. Cost increases occur for equipment and tooling cost categories, with smaller increases for direct and indirect labour costs. Comparison of dedicated and utilisation-based plants running at 20k parts/yr shows a reduced but still significant cost increase of 115% for the dedicated operation. Comparison of

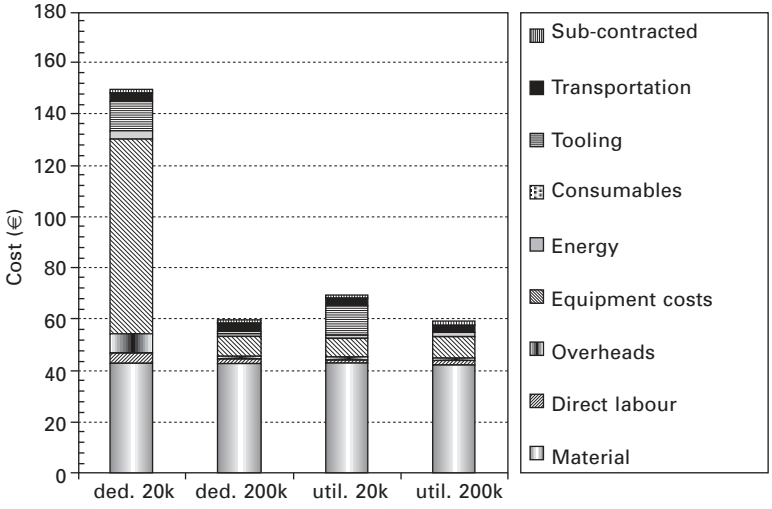

10.14 Effect of plant dedication or utilisation scenario on part cost segmentation versus volume.

utilisation-based plants at 20k and 200k parts/yr shows the same cost levels for all cost categories, with the exception of tooling cost that is always dedicated. Production of 200k parts/yr in a dedicated plant (five years, three-shift pattern) showed only a marginal cost increase of 0.5% versus a utilisation-based line at the same volume. Therefore, dedicated plants should ideally only be considered where close to the production capacity would be used.

Utilisation-based two-plant scenario

In practice, it is difficult to assume an optimised plant layout and still claim a utilisation-based line, because for the remaining 90% capacity a different product would need to be produced that may require a different physical plant layout or dynamics. A two-plant scenario is therefore examined where the stamped fabric part is made in a first factory, which is then shipped (with additional transport and labour costs) to a second factory. The stamped part is then over-moulded and any final trimming or finishing performed, again with additional labour assumed. The stamping cycle time of 50 s enables 307k parts/yr to be produced (three shifts), and hence plant costs for 20k stampings are amortised over a high volume if the stamping sub-supplier is fully utilising the stamping line. As standard machine layouts do not need to be altered to produce the X-brace in two such steps (1st stamping plant and 2nd over-moulding plant), it is particularly suitable for lower volumes and in fact gives lower costs than a dedicated (three-shift) plant up to volumes of 160k parts/yr (Fig. 10.13). From here on, the higher transportation and labour costs of a two-plant scenario are outweighed by the optimised, dedicated

plant. Hence subcontracted two-plant set-ups are the lowest cost alterative for lower manufacturing volumes, while (for this case) dedicated plants are only justified at above 80% plant utilisation.

All sensitivity studies from this point forward consider a one-plant utilisation-based scenario.

10.4.7 X-brace production sensitivity studies

The following section examines the effect of the following examples on GF/PP X-brace production costs (20k parts/yr, three-shift pattern, utilisation-based):

- percentage weight saving *vs*. steel;
- high *vs*. low automation levels;
- high *vs*. low equipment investment;
- 60 s *vs*. 120 s line cycle time;
- material cost (–10% and +10%);
- 2% to 20% reject rates;
- material scrap: hot drape forming, 10% sheet scrap;
- sheet material recycling strategy: 30% scrap with and without recycling;
- labour level: two *vs*. six workers;
- tooling cost (–10% and +10%).

Figure 10.15 plots the baseline X-brace cost and the cost change over the factor range studied in each case. Rather than plotting a simplistic ±% difference to all factors, the difference in each factor that could be expected in reality was compared.

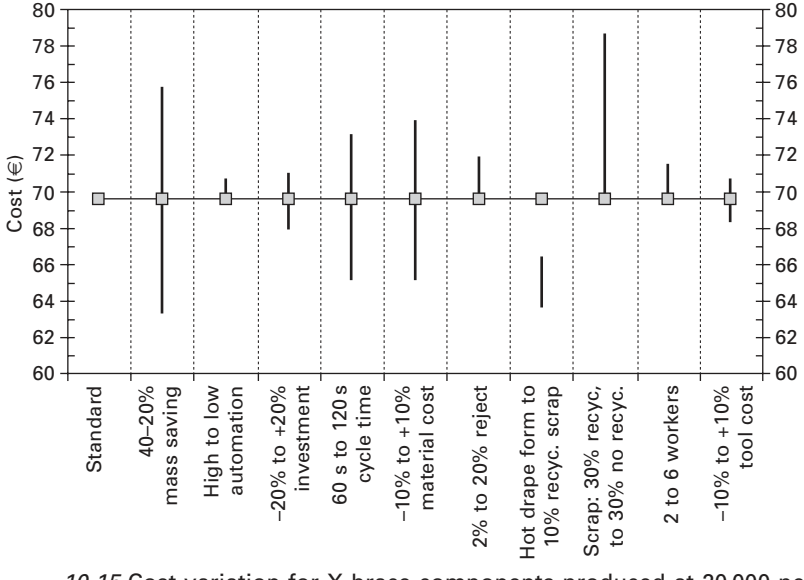

10.15 Cost variation for X-brace components produced at 20 000 per year in GF/PP.

Effect of weight-saved assumption

An important assumption behind TCMs of textile composites is the weight saving that could be expected from using a polymer and composite system, here to replace the current 19 kg steel system. A baseline weight saving of 30% for a GF/PP system was assumed for this study. Full design and FEA simulations would be needed to verify this estimation and hence sensitivity studies have been made of 20–40%, assuming that all the other TCM parameters are unchanged. This change in weight-saving assumption corresponds to costs of €76 and €63 respectively. Figure 10.15 shows that this gives the largest cost variance and that this estimate is hence an important figure, justifying further analysis before any decision for full-scale development. Here the material cost percentage in the overall process was 63%. A lower proportion would reduce the effect of the weight-saving assumption, for example including all the steps in Fig. 10.4. A 30% weight saving has been assumed through the remainder of this study.

Effect of automation level

The effect of the degree of automation was studied by comparing the standard high automation level (two workers and nine robots) with a lower automation level (seven workers and four robots). The lower level increased part cost by 2%. Caution should be used in interpreting these results because the extra hidden set-up costs and higher production engineering overhead costs of the high automation case have not been specifically included. For high-volume industries, the choice of a high or low automation level will depend on the length of a contract from an OEM (original equipment manufacturer) to a Tier 1 supplier such that the capital invested can be recovered in the total production period. Lower automation, with corresponding lower capital costs, and the ability to relocate labour, may create a lower risk for the Tier 1 supplier despite the marginally higher part cost.

Effect of plant investment

The effect of equipment cost on part price was studied by investigating a –20% and +20% variation. Cycle times and scrap rates were assumed constant. This would reflect any estimates made in the necessary equipment capacities or to cover the addition of extra items that were not initially included. This 40% difference caused a 4% shift in part cost, which is a larger effect than a changing automation level. However, the +20% increase in plant cost had a smaller effect than increasing the number of workers, as discussed below.

Effect of cycle time

Increasing the cycle time from 90 s to 120 s decreased the maximum parts/yr from 205k to 153k. With plant costs now amortised over a decreased total number of parts, the part cost increases, with additional increases in direct and indirect labour costs per part. If the plant were running at maximum capacity, the tooling costs per part would also increase. Decreasing the cycle time to 60 s increased the maximum annual production rate to 307k parts/yr. Between 120 s and 60 s a cost reduction of 11% (€7.2) occurred, showing that cycle time is a parameter of key importance towards reducing part cost, provided that scrap and reject rates are not affected.

Effect of raw material price

The effect of raw material cost (both sheet material and over-moulding material) on part price was studied by investigating a –10% and +10% variation. A smaller difference was assumed compared with plant cost due to increased confidence in the quotations. As expected for a process where material costs form 63% of the total cost, changing raw material costs had an important effect, with the part price ranging from €65.2 with a –10% material cost to €73.8 at a +10% material cost (a 13% change). Hence, material cost for such textile composite processes is an important issue, notably if higher added-value sheet materials were used.

Effect of reject rate

Reject rate refers to parts at the end of the production line that cannot be sold. If a part becomes rejected at an earlier stage in the process, less value is lost than if rejected at the end of the line. When a part is rejected, it is assumed that new material and additional machine time in all process steps preceding the reject decision are needed to replace it. Rejected part costs are hence compounded through the process steps. Rework of rejected parts is not assumed. Reject parts can be sold as material for recycling, where payment is received, or a cost may be incurred to pay for removal. Here rejected parts are assumed cost neutral in terms of sale or disposal. While high-volume thermoplastic forming and over-moulding processes are relatively stable (when established), other lower-volume textile processes (with reduced plant investment) may have higher reject rates and hence the effect of 20% rejected parts is shown, increasing part cost by 3%. As Fig. 10.15 shows, higher reject rates have an important effect, such that if the +20% plant investment referred to above were to reduce reject rates, then the increased plant costs would be justified.

Recycling strategy

Owing to the high stamped sheet cost percentage, the effect of the percentage sheet that is trimmed from the stamped part before over-moulding is shown. Scrap results when:

- the developed part surface is not rectilinear (the difference between the developed shape and the rectilinear blank is waste, Fig. 10.16a);
- material is held by a blank-holder during the stamping process that is not part of the final component.

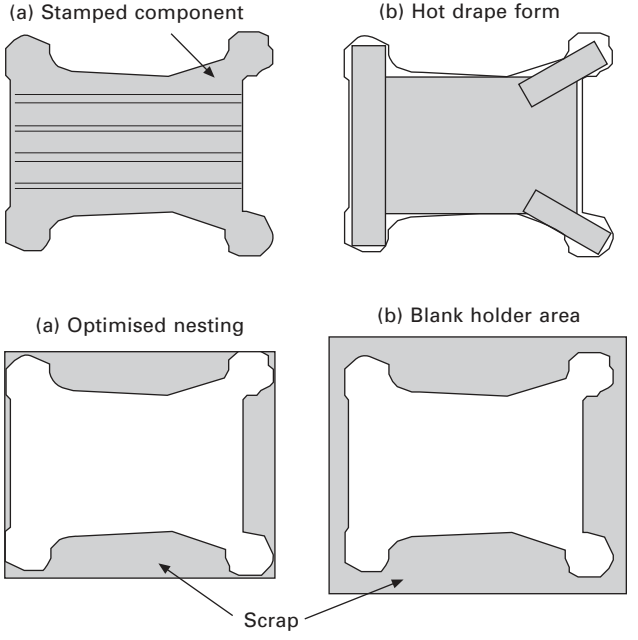

10.16 Textile composite scrap for different blank layouts.

The standard stamped sheet waste allocated here is 30% (Fig. 10.16d). Additional stamped sheet is therefore specified to give that required for the part while leaving an additional 30% scrap. The scrap is directly reused, with additional virgin granules to adjust the fibre fraction, in the over-moulding process. While a closed loop recycling solution is proposed here, the stampable sheet is more expensive than virgin injection moulding pellets.

The first comparison compares: a scenario where the stamping scrap is not recycled but can be essentially eliminated, and a low stamping scrap percentage of 10% (recycled in-line). Stamping waste could be eliminated if the sheet area were inside the part edges (Fig. 10.16b). Pre-consolidated sheet would be heated and then hot draped to the tool geometry using a

lower-cost shaping tool, and placed locally in the mould where it is needed. Hence a separate stamp-forming stage would not be used, reducing tool and press costs. A limitation would be that structural sheet would not span the whole component, notably at non-linear edge regions. A 10% stamping scrap scenario would represent optimised 'nesting', here shown as an example with the equivalent rectilinear blank minus the final part shape (Fig. 10.16c). Both the hot-drape forming and 10% scrap scenarios reduced costs by 9% and 5% compared with the standard 30% scrap. The 10% scrap scenario would keep full fabric placement freedom and therefore a choice between the processes will be driven by a combination of part design and achieving the lowest manufactured part price.

To show the effect of closed-loop recycling that is possible with the GF/PP stamped textile sheet, costs were compared for 30% stamping scrap (giving material area for a blank-holder that controls fabric deformation to the mould) both with and without recycling. Equipment costs were marginally reduced without recycling while less over-moulding material was needed where the grinding machine was used. Elimination of in-line recycling increased part cost by 13% (€9.2). In this case, in-line recycling is clearly advantageous.

Effect of operator level

The standard layout allocated two workers to run the line. Without detailed knowledge of the process, gained through experience and process-flow simulations, specification of the exact number of operators is difficult. Hence the operator level was increased to six, with a corresponding cost increase of 3%. This was greater than the effect of increasing the plant cost by 20%. Similar attention should therefore be paid to controlling the operator levels as to optimising plant investment. A larger effect would occur in a dedicated plant running at below the maximum capacity for any given shift pattern.

Effect of tooling cost

The final comparison made is that of tooling cost. If, for example, sliding cores are needed, or a choice of materials/surface treatments (chrome plated *vs*. polished steel *vs*. surface texture) must be made, then tooling costs may vary during the development of a component. Here a –10% to +10% variation gave a cost difference of 3% for a manufacturing volume of 20k, decreasing to a difference of below 0.5% at 200k parts/yr. For lower manufacturing volumes, tooling costs should be more carefully controlled, while for high manufacturing volumes tooling costs are amortised over an increased number of parts and tooling should be optimised for performance.

10.5 Case study 2: composites for the Airbus family

10.5.1 Introduction

The demand for weight saving in aerospace applications, with a lower sensitivity to production rates and material costs, has led to the development of composite processing techniques that can achieve both cost and weight reduction when a system approach is taken. The first composite primary structure to enter production on a commercial aircraft was the A300/A310 CF/epoxy prepreg composite rudder[32]. This replaced its metal counterpart without design changes to the aircraft, reducing 2000 parts (including fasteners) for the metal system to fewer than 100 for the composite system with a 20% weight saving, and an overall cost saving, despite the higher raw material cost. Combined with other design changes, the composite rudder and vertical fin lead to reduced fuel consumption.

Airbus and Fokker have demonstrated cost reductions through using thermoplastic textile composites. For example, giving a total of 1000 kg of textile thermoplastic composites per aircraft, the Airbus A340-500/600 incorporates: engine pylon panels, keel beam ribs and profiles, lower wing access panels, the inboard fixed wing leading edge and aileron ribs. Such textile materials (CF/PPS, polyphenylsulfone), used for example in rib manufacturing (for 16 ribs), have shown similar costs to metallic structures with €95 for aluminium versus €125 for CF/PPS produced by rubber stamp-forming. However, a weight reduction for CF/PPS compared with the metallic structure was valued at an additional cost of €285 for the metallic structure, giving an effective cost saving for the CF/PPS parts. CF/PPS showed a 90% cost reduction compared with prepreg materials and autoclave processing (€245), for the same overall weight[33].

10.5.2 Composite material systems for A380 fuselage panels

The second case study, using data supplied by Airbus[34], focuses on the Airbus A380 that in passenger configuration seats 550–650 people (mixed-class) by using an oval cross-section with a double-deck cabin configuration (full aircraft length). To minimise airport infrastructure modifications, the wingspan and aircraft length were required to fit within an 80×80 m^2 box. Maximum outer dimensions of the fuselage are 7.2 m wide by 8.6 m high. The following candidate carbon fibre reinforced epoxy composite material systems are compared for A380-family fuselage panels aft of the rear pressure bulkhead, as shown in Fig. 10.17[34]:

- hand lay-up of pre-impregnated woven fabrics;

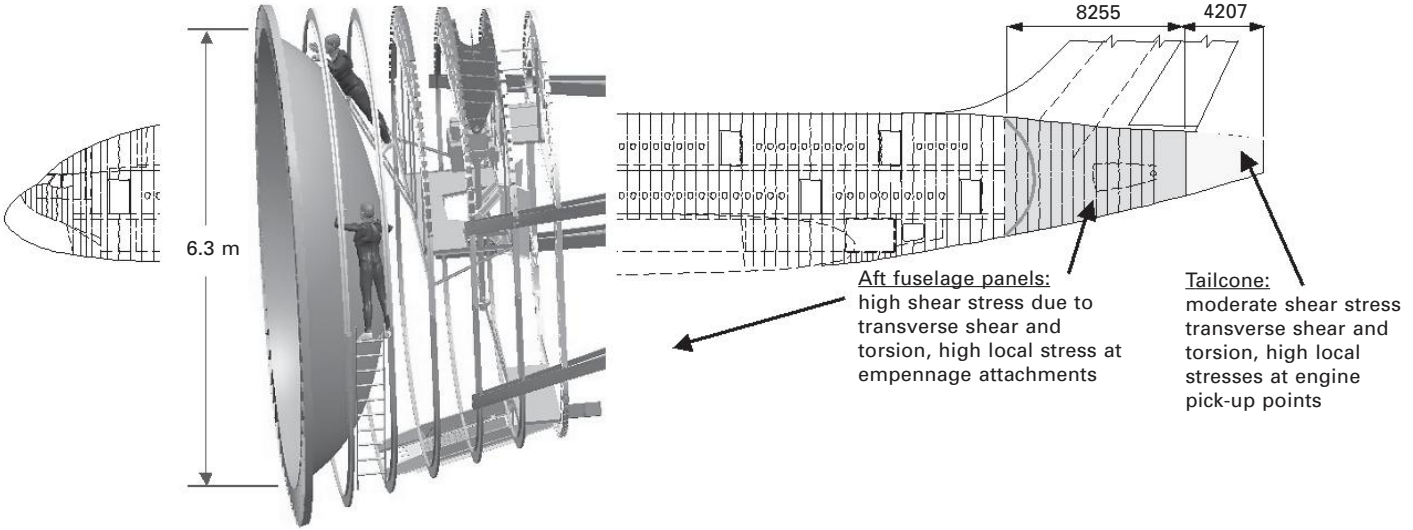

10.17 Airbus A380 structural design for aft fuselage (adapted from Hinrichsen[34]).

- hand lay-up of dry fabrics (for resin film infusion);
- automated tape laying (ATL) (pre-impregnated tapes);
- automated fibre placement (AFP) (pre-impregnated slit tapes/tows).

Panel size and the number of joints needed for fuselage shells are important parameters that determine both weight and manufacturing costs. The large size of the A380 fuselage requires materials and manufacturing processes for longer and wider panels at twice the average thickness compared with smaller aircraft (A320 and A340). 'Design for maintainability' (repairs after tail-strike events) requires that the panel arrangement and additional frame joints allow exchange of lower fuselage structure elements using spare part kits, independent of material and manufacturing process selection. Another parameter for the selection process is the complex aerodynamic shape of the aft-fuselage, affecting the number of panels and joints. Restrictions of metal stretch-form operations for strongly double-curved geometries limit panel sizes and consequently increase the number of panel joints compared with a composite design solution. The aft-fuselage shape also has a strong impact on manufacturing process selection for composite panels.

10.5.3 Material costs

The four composite material systems were compared for the aft-fuselage panels based upon the material costs associated with the manufacture of 1 kg of flying structure. The material cost consists of the material purchase price and the material overhead costs (which in this study is 5% covering all costs linked to purchase activities and acceptance control on delivery and storage). The material cost is segmented into the allocated material overhead costs, material waste costs and the flying material cost, as shown in Fig. 10.18. The lowest material cost occurred for hand lay-up of dry fabrics. It can be seen that waste is an important fraction of the material costs, which is lowest for AFP. Waste occurs principally during pre-form cutting, resulting in unusable pieces of pre-impregnated woven fabrics, and during final edge trimming of the cured lay-up. The waste assumptions made here reflect the large fuselage panel application in combination with state-of-the-art materials handling and different buy-to-fly (B/F) ratios would apply for different geometries and applications.

10.5.4 Manufacturing process performance

With a target annual production rate of 48 aircraft/year, and with six panels per unpressurised fuselage, the annual panel production rate is 288 per year, representing a lower annual rate compared with the case study in section 10.4. The panel arrangement for a composite solution achieves cost savings

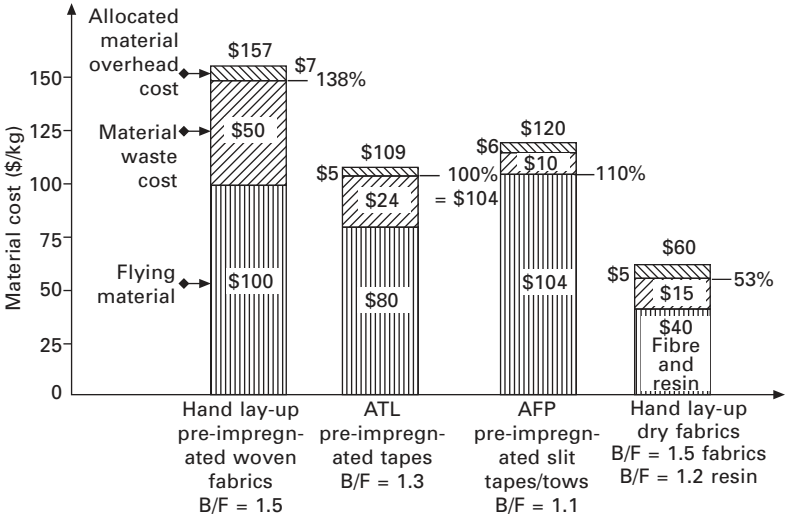

10.18 Airbus A380 aft fuselage material cost comparison (adapted from Hinrichsen[34]).

primarily through a reduction in the number of joints. Simulation of lay-up for the four processes revealed that ATL was not suitable due to the degree of double curvature. The required split into four large panels was feasible for both AFP and hand lay-up. Both hand lay-up processes had adequate access to the female mould for the worker, with deposition rates of 1.6 kg/h, but eventually this would be constrained by the mould size. AFP is less constrained by the size of the male tool and for skin manufacture is suited to 2–4.7 kg/h rates. However, AFP is also constrained by subcomponent size as the uncured skin is transferred into a female tool for stringer placement prior to the cure cycle, where stringer positioning requires equivalent accessibility as for hand lay-up.

Using the above deposition rates for each process and introducing costs for labour and equipment, scatter-bands for 'process cost' versus 'complexity' were established, as shown in Fig. 10.19. A charge rate of $500/h was assumed to cover the costs related to the AFP-machine at average utilisation, including supervision. For the hand lay-up processes, a charge rate of $80/h was used, including all costs for workforces and the use of shop-floor facilities. All costs are recurring costs, including all work linked to the delivery of uncured *skins* for fuselage panels ready for positioning stringers on the delivered lay-up, which occurs in a further process. Hence, materials and manufacturing costs are defined as recurring cost per kg flying structure.

Figure 10.19 enables the manufacturing process cost to be determined versus degree of complexity, depending on the deposition rate. The triangular symbols indicate average deposition rates based upon the aft-fuselage panel

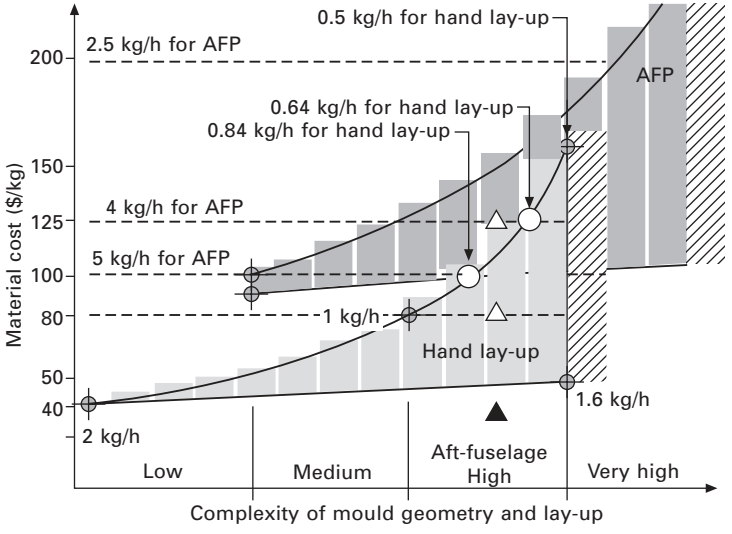

10.19 Process cost comparison for Airbus A380 aft fuselage (adapted from Hinrichsen[34]).

complexity and hence $/kg cost values for hand lay-up and AFP processes. As hand lay-up of dry fibres (e.g. NCFs for the resin film infusion process) requires additional time compared with hand lay-up of pre-impregnated fabrics, a lower kg/h rate is used, indicated by circular symbols. This is due to the difficulties of placing dry fibres with the right accuracy, and the fact that resin film has to be arranged between the fibre layers.

The combined material and process costs, valid for the delivery of uncured skins, are summarised in Table 10.6. Hand lay-up of prepregs and AFP end up at equal cost, whereas the lay-up for the RFI process yields savings in the order of 25%, despite the fact that labour costs are 50% higher compared with hand lay-up of prepregs. It can be seen that, except for the resin film approach, material costs form 50% of the total cost linked to the delivery of laid-up skins. For hand lay-up of woven fabrics, half of these material costs are due to waste, showing the prime driving force for AFP.

Table 10.6 A380 aft-fuselage panel material and process costs

	Hand lay-up, pre-impregnated fibres ($/kg)	AFP ($/kg)	Hand lay-up, dry fibres ($/kg)
Material	157	120	60
Labour	80		120
Machine	–	125	–
Total	237	245	180

10.5.5 Assessment on an aircraft section level

A comparison of panel materials requires comparison over an aircraft section. The conventional all-metal design with Al2524 panel skins, Al7075 stringers and Al7050 milled frames, served as a reference. Composite materials were assumed to replace both aluminium panels and sheet metal frames, but with both metallic and composite panel solutions sharing 36% weight common metal parts.

Composite materials reduced the total weight by 15%, while also decreasing the panel count from 16 aluminium panels to four carbon fibre reinforced polymer (CFRP) panels. This reduced assembly costs from 17% total for the metallic solution to 12% total for composite. Cost per unit mass was estimated by considering the uncured panel cost, the curing costs, finishing costs and assembly costs. For finished (cured) CFRP parts substituting metal parts, this was estimated as $300/kg, the common metal parts as $220/kg, and for the metal parts competing with CFRP, $250/kg. Relative costs and weights are compared in Fig. 10.20 for the two materials. Costs for metal panels were 11% higher than composite panels due to high waste fractions for each of the 16 panels resulting from stretch-forming, the high price of advanced aluminium alloys, and the subsequent assembly of 16 metallic panels with the associated labour-intensive forming and heat-treatment operations.

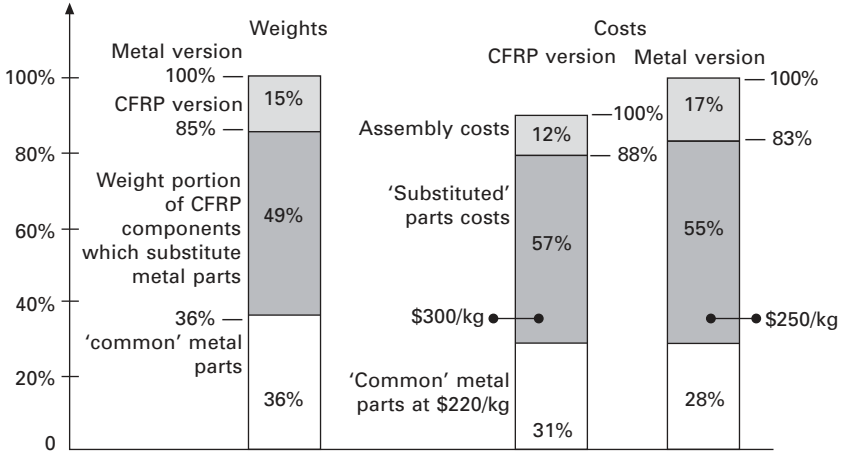

10.20 Airbus A380 aft fuselage cost assessment on an aircraft section level (adapted from Hinrichsen[34]).

Consideration of the system cost hence gives an 11% cost reduction for CFRP using either hand lay-up or AFP, together with a 15% weight saving. The weight saving will reduce fuel usage thereby decreasing aircraft operational costs during the product life cycle, while achieving a lower initial construction cost.

10.6 Conclusions

The TCM approach has been shown to offer a route to assess the cost of textile composite structures to include the effect of fibre type, matrix resin, prepregging route, conversion technique, scrap and waste management, finishing and assembly. Where the system cost is considered, textile composite structures were shown through two case studies to offer cost reductions compared with metallic references. The reduction of scrap in textile composite processing was shown to be of high importance. Tooling cost was also shown to be an important issue, notably where metallic tools are needed for lower production volumes. The strategic consideration of manufacturing plant utilisation or dedication was shown to be a key assumption in cost calculations in situations where the manufacturing supply base is still being established. Materials and processing techniques should be considered together from the outset to suit the desired manufacturing volume and the cost structure of the application market sector.

10.7 Acknowledgements

The authors wish to acknowledge funding from the many anonymous research projects that have enabled the creation of modelling tools and case study data that have been generalised into the material in this chapter. Colleagues at the EPFL and IMD including F. Roduit, C. Menzl, A. Mahler, H. Hermann, Dr P. Sunderland, N. Weibel, N. Mona, K. Becheler and Prof. T. Vollmann are also thanked for their research collaboration. Industrial contacts who have provided information specifically for this chapter include: Dr P. Blanchard (Ford Motor Company), Mr J. Hinrichsen (Airbus), Mr W.V. Dreumel (TenCate Advanced Composites), Mr D. Cripps (SP systems), Mr P. Lucas (Vetrotex International), Mr M. Schrief and Mr. T. Bischoff (Saertex), and Mr I. Toll (Aeroform Ltd). The authors also wish to thank the many anonymous industrialists who have contributed to the cost modelling approach and the data presented in this chapter.

10.8 References

1. Wakeman M.D., Bonjour F., Bourban P.E., Hagstrand P.O. and Månson J.A.E., 'Cost modelling of a novel manufacturing cell for integrated composite processing', *23rd International SAMPE Europe Conference*, Paris, France, 9–11 April 2002.
2. Bernet N., Wakeman M.D., Bourban P.E. and Månson J.A.E., 'An integrated cost and consolidation model for commingled yarn based composites', *Composites Part A*, 2002, 33, 495–506.
3. Wakeman M.D., Sunderland P.W., Weibel N., Vollmann T. and Månson, J.-A.E., 'Cost and implementation assessment illustrated through composites in the automotive industry – part 1: methodology', in preparation, 2005.

4. Weibel N.D., Sunderland P.W., Wakeman M.D., Månson J.A.E., Vollmann T.E. and Bechler K., 'Beyond a cost model: assessing implementation of new materials technologies', *10th International Conference on Management of Technology IAMOT*, Paper 231NW, Lausanne, 2001.
5. Weibel N.D., Sunderland P.W., Wakeman M.D., Vollmann T.E. and Månson J.A.E., 'Beyond a cost model: assessing implementation of new composite technologies', *J. Cost Management*, 2002, 16/3, 21–29.
6. Silverman E.M. and Forbes W.C., 'Cost analysis of thermoplastic composites processing methods for spacecraft structures', *SAMPE J.*, 1990, 26(6), 9–15.
7. Walls K.O. and Crawford R.J., 'The design for manufacture' of continuous fibre-reinforced thermoplastic products in primary aircraft structures', *Compos. Manuf.*, 1995, 6(3–4), 245–254.
8. Bader M.G., 'Materials and process selection for cost-performance effective laminates'. *Proceedings of the Eleventh International Conference on Composite Materials*, Gold Coast, Australia, 1997, 621–629.
9. Gutowski T., Henderson R. and Shipp C., 'Manufacturing costs for advanced composites aerospace parts', *SAMPE J.*, 1991, 27(3), 37–43.
10. Karbhari V.M. and Jones S.K., 'Activity-based costing and management in the composites product realization process', *Int. J. Mater. Prod. Technol.*, 1992, 7(3), 232–244.
11. Mayer C., Hartmann A. and Neitzel M., 'Cost-conscious manufacturing of tailored thermoplastic composite intermediates using a double belt press', *Proceedings of the 18th International SAMPE Europe Conference*, Paris, France, 1997, 339–351.
12. Wang E. and Gutowski T., 'Cost comparison between thermoplastic and thermoset composites', *SAMPE J.*, 1990, 26(6), 19–26.
13. Foley M. and Bernardon E., 'Thermoplastic composite manufacturing cost analysis for the design of cost effective automated systems', *SAMPE J.*, 1990, 26(4), 67–74.
14. Gutowski T., Hoult D., Dillon G., Neoh ET., Muter S., Kim E. and Tse M., 'Development of a theoretical cost model for advanced composite fabrication', *Compos. Manuf.*, 1994, 5(4), 231–239.
15. Kang P.J., 'A technical and economic analysis of structural composite use in automotive body-in-white applications', MSc Thesis, Department of Materials Science and Engineering, Massachusetts Institute of Technology, 1998.
16. Marti H.G., 'The cost modeling of automotive body-in-white assembly using relational databases', BSc Thesis, Department of Materials Science and Engineering, Massachusetts Institute of Technology, June 1997.
17. Kirchain R.E., 'Modeling methods for complex manufacturing systems: studying the effects of materials substitution on the automobile recycling infrastructure', PhD thesis, Department of Materials Science and Engineering, Massachusetts Institute of Technology, Feb. 1999.
18. Lee D.E. and Hahn H.T., 'Virtual assembly production analysis of composite aircraft structures', *Proceedings of the 15th International Computing Engineering Conference and the 9th ASME Engineering Database Symposium*, Boston, USA, 1995, 867–874.
19. Jones S.C., 'Profit Cue^{TM} (process-fitted cost and quality evaluator)', CompositeTechBrief N^{o} 103, Center for Composite Materials, University of Delaware, Newark, USA, 1997.
20. Li M., Kendall E. and Kumar J., 'A computer system for lifecycle cost estimation and manufacturability assessment of composites', *Proceedings of the Eleventh*

International Conference on Composite Materials, Gold Coast, Australia, 1997, 630–639.
21. Olofsson K. and Edlund A., 'Manufacturing parameter influences on production cost' submitted for publication at the, *International Conference on Advanced Composites, SICOMP Technical Report* 98–009, 1998.
22. Evans J.W., Mehta P.P. and Rose K., 'Manufacturing process flow simulation: an economic analysis tool', *Proceedings of the 30th Int. SAMPE Technical Conference*, San Antonio, USA, 1998, 589–595.
23. Kendall K., Mangin C. and Ortiz E., 'Discrete event simulation and cost analysis for manufacturing optimisation of an automotive LCM component', *Composites Part A*, 1998, 29A(7), 711–720.
24. Clark J.P., Roth R. and Field F.R., 'Techno-economic issues in materials selection', in *ASTM Handbook, vol. 20*, Materials Selection and Design, 1997, 256–265.
25. Rampersad H.K., *Integrated and Simultaneous Design for Robotic Assembly*, John Wiley & Sons, Inc. 1994.
26. Månson J.-A.E., Wakeman M.D., Bernet N., 'Composite processing and manufacturing – an overview', in *Comprehensive Composite Materials*, Ed. Kelly A. and Zweben C., Vol 2, 577–607, Elsevier Science, Oxford, 2000.
27. Johnson C.F. and Rudd C.D., in Kelly A. (ed.), *Comprehensive Composite Materials*, Elsevier, 2000, Cht. 2.32, 1049–1072.
28. Månson J.A.E., Bourban P.E. and Bonjour F., 'Process and equipments for the manufacture of polymer and for composite products', European Patent Office, EP 0825 922 B1, 17 May 1996.
29. Luisier A., Bourban P.E. and Månson J.A.E., 'Time–temperature-transformation diagram for reactive processing of polyamide 12', *J. Appl. Polymer Sci*., 2001, 81, 963–972.
30. Wakeman M.D., Zingraff L., Kohler M., Bourban P.E. and Månson J.A.E., 'Stamp-forming of carbon fiber/PA12 composite preforms', *Proceedings of the Tenth European Conference on Composite Materials*, 3–7 June 2002, Brugge, Belgium.
31. Zingraff L., Bourban P.E., Wakeman M.D., Kohler M. and Månson J.A.E., 'Reactive processing and forming of polyamide 12 thermoplastic composites', *23rd SAMPE Europe International Conference,* Paris, France, 9–11 April, 2002.
32. Anon, 'A brief look at composite materials in Airbus commercial aircraft', *High Performance Composites*, March/April 1999, 32–36.
33. Mr. Dreumel W.V., 'Personal communication', TenCate Advanced Composites, November 2002.
34. Hinrichsen J., 'A380 – the flagship for the new century', Proceedings of JISSE-7, Japan, 2001.